國立交通大學

光電工程研究所

碩 士 論 文

使用GHz鎖模光纖雷射來產生超連續光源之研究

Supercontinuum generation using a GHz Mode-locked Fiber Laser

研 究 生：葉人豪

指導教授：賴暎杰　教授

中 華 民 國 九 十 五 年 七 月

使用 GHz 鎖模光纖雷射來產生超連續光源之研究

Supercontinuum generation using a GHz Mode-locked Fiber Laser

研 究 生：葉人豪　　Student：Jen-Hao Yeh

指導教授：賴暎杰　教授　Advisor：Dr. Y. Lai

國 立 交 通 大 學

電機資訊學院　　光電工程研究所

碩 士 論 文

A Thesis

Submitted in Partial Fulfillment of the Requirements for the Degree of Master in The Institute of Electro-Optical Engineering College of Electrical Engineering and Computer Science National Chiao-Tung University

July 2006

Hsinchu, Taiwan, Republic of China

中華民國九十五年七月

使用 GHz 鎖模光纖雷射來產生超連續光源之研究

研究生: 葉人豪　　指導教授: 賴暎杰　教授

國立交通大學光電工程研究所碩士班

摘要

我們利用一 GHz 等級高功率短脈衝的非同步鎖模光纖雷射，配合光纖放大器/脈衝壓縮器，和一段高非線性光纖來產生超連續光譜，此超連續光譜可涵蓋從 1120 nm 到超過 1800 nm 的波段。此系統的第一級光源爲一功率爲 14 mW、脈衝寬度爲 1.8 ps、重複率爲 1 GHz 的脈衝序列。之後，我們用一光纖放大器來提高光功率至 1.2 W 並同時將脈衝寬度壓縮至 414 fs。最後，我們將此脈衝序列入射至一段長 0.95 m 的高非線性光纖來產生超連續光譜。這種高重複率等級的超連續光源應能應用在諸如頻譜量測、頻率標準等之許多領域。

Supercontinuum generation using a GHz Mode-locked Fiber Laser

Student: Jen-Hao YEH Adviser: Professor Yinchieh Lai

Department of Photonics & Institute of Electro-Optical Engineering

College of Electrical Engineering and Computer Science

National Chiao Tung University

Abstract

We demonstrate a high power short pulse-width light source composed of a 1GHz asynchronous modelocked (ASM) fiber laser, an Er-Yb optical amplifier/pulse compressor, and a section of high nonlinearity fiber (HNLF) to generate supercontinuum lights with the spectrum span from 1120 nm to over 1800 nm. The ASM fiber laser generates 1.8 picosecond pulses with 14 mW average power at 1 GHz repetition rate. After amplification, about 1.2W average power of 414 femtosecond pulses are generated. Finally, we launch the pulse train into a HNLF with the length of 0.95 m to generate the supercontinuum. This kind of high repetition rate supercontinuum light sources will potentially have lots of applications including spectral measurement and frequency metrology.

Acknowledgement

經過兩年的碩士班生活，我學到了許多東西，這段期間仰賴了很多人的幫忙，讓我能順利完成此論文。

感謝賴暎杰老師對我各方面的指導，不只增進了我的知識，也讓我學到了作研究的方法與態度以及求知的精神。感謝項維巍學長於實驗上的指導，讓我能迅速進入狀況，順利地進行實驗。感謝祁甦老師，陳智弘老師以及林炆標老師撥空擔任口試委員，並給了我許多寶貴的建議。

同時也感謝電資 501 實驗室的各位學長：林俊廷學長，彭朋群學長，馮煒仁學長，錢鴻章學長於實驗器材上的借助與指教。另外也感謝徐桂珠學姊，周森益學長，邱鐘响同學於實驗上的討論及課業上的幫忙。

最後，感謝母親與弟弟的支持與鼓勵，還有朋友們的關心，僅以此篇論文與各位分享我的喜悅之情。

2006.07.15 交大

Contents

Contents of Figures

Chapter 1 Introduction

1.1 Introduction of supercontinuum generation

Supercontinuum generation means the broadening of a relatively narrow spectral bandwidth of a laser into a broad bandwidth, typically spanning an optical octave or more. The first experiment was demonstrated by Alfano and Shapiro in 1970 and they reported the generation of a 200 THz-wide continuous spectrum of light in bulk glass [1]. Similar result was observed in H_2O and D_2O in 1977 [2] and in a jet stream of gaseous ethylene glygol in 1983 [3]. In the case of optical fibers, supercontinuum generation was first observed using a multimode fiber [4], and later on, it was achieved in a conventional single-mode optical fiber in 1987 [5]. Several fiber designs have been proposed to enhance the generated bandwidth. A bandwidth of a few hundred nanometers was obtained by decreasing the dispersion along the fiber at the telecommunication wavelengths [6]. With newly invented microstructure photonic crystal fibers, the spectral broadening is so pronounced that the resulting frequency comb can span more than an optical octave. Supercontinuum generation is a complex nonlinear process by using a spectral broadening of light pulses propagating through a nonlinear medium. Generally speaking, they are generated in micron scale air-sillica wave guides pumped by fs Ti-Sapphire lasers near 800nm [7], and infrared supercontinua are produced using erbium-doped femtosecond fiber lasers and germano-silicate highly nonlinear dispersion shifted fiber [8]. In recent years, lots of experiments used pulsed [9][10] or continuous wave

(CW) [11][12] light source launched into microstructure or tapered optical fibers as well as high nonlinear fiber (HNLF) to generate the continuum. Its broadband and ultrashort characteristics make it a unique light source for numerous novel applications in the field of telecommunication [13], optical metrology [14] and medical science. There are also lots of researches applying supercontinuum sources in dense wavelength-division multiplexing (DWDM) transmission, and a gighertz-repetition rate broadband source may also be useful for high-capacity WDM light-wave transmission systems. By slicing the broad spectrum of the supercontinuum into hundreds of channels, and utilizing an optical time domain multiplexing technique for each channel, transmission bandwidths of terahertz can be achieved [15]. Also the use of a supercontinuum in single-shot characterization of fiber-optic components has been demonstrated [16].

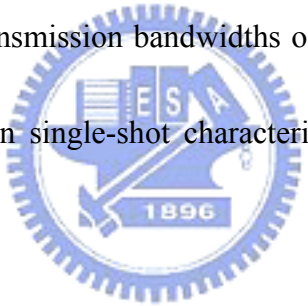

1.2 Motivation

In the literature, most of the reported experiments for supercontinuum generation are performed at low repetition rates (several tens MHz to hundred MHz). In this work, we demonstrate it at the 1GHz repetition rate, which should potentially have some advantages for applications such as frequency metrology. We use our previously developed asynchronous mode-locked (ASM) fiber laser operating at 1GHz repetition rate as the first stage light source and launch its output pulses into a high power optical amplifier for raising the average power

and for pulse compression simultaneously. After amplification, we use single mode fiber (SMF) to compensate the chirp for pulse compression and launch the pulses into HNLF to generate supercontinuum lights. This approach should be able to provide us a high repetition rate supercontinuum light source.

1.3 Outline of the thesis

There are four chapters in this thesis. In Chapter 1, we introduce the background and our motivation for doing this research. Chapter 2 is the theory for the first stage light source – ASM fiber laser and for the mechanisms of optical amplification, pulse compression, and supercontinuum generation. Chapter 3 shows our experimental setup and results. The final chapter gives the conclusions and discusses the possible future work that can be done.

Chapter 2 Principles of the Experiment

Supercontinuum generation requires the interaction of intense pulses with a nonlinear medium. When ultrashort optical pulses pass through a nonlinear medium, some nonlinear effects such as self-phase modulation (SPM), cross-phase modulation (XPM), stimulated Raman scattering (SRS), and four-wave mixing (FWM) will occur. All of these nonlinear processes are capable of generating new frequencies, and the combination of them leads to the optical spectrum broadening. Hence, we will briefly introduce these nonlinear effects in optical fibers first. In addition, it is obvious that the peak intensity of the input pulses will strongly affect the output supercontinuum bandwidth. In order to generate broadband supercontinuum lights at the 1GHz repetition rate, we choose to use a high intensity short pulse light source composed of a mode-locked fiber laser operating at the 1GHz repetition rate and a high power optical amplifier for power amplification and pulse compression simultaneously. Therefore, we will also introduce the principles of optical amplification/pulse compression and mode-locked laser in the later sections of this chapter.

2.1 Nonlinear effects in optical fibers

The propagation of single polarization light pulses in optical fibers can be described by the following propagation equation derived from the general wave equation [17, Chapter 2.1] :

$$\nabla^2 E - \frac{1}{c^2}\frac{\partial^2 E}{\partial t^2} = -\mu_0 \frac{\partial^2 P}{\partial t^2} \tag{2.1.1}$$

where E is the electric field, P is the induced medium polarization, and μ_0 is the vacuum permeability. The induced polarization contains the linear part P_L and the nonlinear part P_{NL} which becomes considerable for intense pulses. Under the scalar approximation, P_L and P_{NL} can be related to the electric field：

$$P_L = \varepsilon_0 \chi^{(1)} E \tag{2.1.2}$$

$$P_{NL} = \varepsilon_0 \chi^{(k)} E^k \tag{2.1.3}$$

where ε_0 is the vacuum permittivity, and $\chi^{(k)}$ is the k-th order susceptibility. For silica, the even-order susceptibility can be negligible because of the centro-symmetric property of the material. Furthermore, susceptibility of order higher than 3 are very small and usually can be neglected. Therefore the nonlinear effects we are going to discuss are the parts induced by the third-order susceptibility $\chi^{(3)}$. Some nonlinear effects are elastic processes in which there is no energy exchange between the electromagnetic fields and the material. These effects include the SPM, XPM and FWM. Other kinds of nonlinear effects are inelastic processes including the SRS and SBS, in which there is the energy exchange between the electromagnetic fields and the material.

One can derive the nonlinear equation which describes the propagation of lights along optical fibers by considering the nonlinear part of the induced polarization as a perturbation and the result is a high-order differential equation [17, Chapter 2.3]：

$$\frac{\partial A}{\partial z}+\frac{\alpha}{2}A+\beta_1\frac{\partial A}{\partial t}+\frac{i\beta_2}{2}\frac{\partial^2 A}{\partial t^2}-\frac{\beta_3}{6}\frac{\partial^3 A}{\partial t^3}$$
$$=i\gamma\left(1+\frac{i}{\omega_0}\frac{\partial}{\partial t}\right)\left(A(z,t)\int_{-\infty}^{\infty}R(t')\left|A(z,t-t')^2\,dt'\right|\right) \quad (2.1.4)$$

where A represents the slowly varying envelope of the electric field at the carrier frequency ω_0, α is the fiber attenuation, γ is the nonlinear coefficient, and β are the coefficients of the Taylor series expansion of the propagation constant in the frequency domain. *R(t)* is the response function of the nonlinearity including both the electronic and vibration contributions and is defined as：

$$R(t)=(1-f_R)\delta(t)+f_R h_R(t) \quad (2.1.5)$$

Where f_R represents the fractional contribution of the delayed Raman response to the nonlinear polarization P_{NL}, and $h_R(t)$ is the Raman response function.

In the following sections, special notice is paid to the nonlinear effects of importance in this work including the SPM, XPM, FWM, SRS and SBS. The basic principles of these effects will be briefly introduced.

2.1.1 Self-Phase Modulation (SPM)

Self-phase modulation, a phenomenon that leads to spectral broadening of optical puses, is the temporal analog of self-focusing. The refractive index of a fiber can be written as the following equation by taking into account the intensity-dependence [17, Chapter 2.3]：

$$n=n_0+n_2 I \quad (2.1.6)$$

where I is the optical intensity in the fiber, n_0 is the linear part of the refractive index and n_2 is the nonlinear index coefficient defined by

$$n_2 = \frac{3}{8}\frac{1}{n_0}\mathrm{Re}\left(\chi^{(3)}\right) \tag{2.1.7}$$

The n_2 is related to the nonlinear parameter γ described by：

$$\gamma = \frac{n_2\omega}{cA_{eff}} \tag{2.1.8}$$

where ω is the carrier frequency and A_{eff} is the effective area of the mode propagating inside the optical fiber which is defined as：

$$A_{eff} = \frac{\left(\int_{-\infty}^{\infty}\int |F(x,y)|^2 dxdy\right)^2}{\int_{-\infty}^{\infty}\int |F(x,y)|^4 dxdy} \tag{2.1.9}$$

Here $F(x,y)$ means the fundamental fiber mode profile. The A_{eff} depends on the fiber parameters including the core radius and the core-cladding index difference. If $F(x,y)$ is approximated by a Gaussian distribution, the effective area can approximated by $\pi\rho^2$ with ρ being the radius of the fiber core [18].

The SPM is a direct consequence of the intensity dependence of the refractive index of silica. The main effects of SPM can be understood by considering only the first term on the right hand side of the equation (2.1.4) with $f_R = 0$ in equation (2.1.5) and with the dispersion terms all neglected：

$$\frac{\partial U}{\partial z} = \frac{i}{L_{NL}}e^{-\alpha z}|U|^2 U \tag{2.1.10}$$

where L_{NL} is the nonlinear length defined as $L_{NL} = (\gamma P_o)^{-1}$ with P_0 being the peak power of

the input pulse. The U is the normalized amplitude and is related to A by $U = A/\sqrt{P_0}e^{\alpha z}$ such that equation (2.1.10) has the solution：

$$U(z,t) = U(0,t)e^{i\phi_{NL}} \tag{2.1.11}$$

Here ϕ_{NL} is the induced nonlinear phase shift and can be described by：

$$\phi_{NL}(z,t) = |U(0,t)|^2 \frac{L_{eff}}{L_{NL}} \tag{2.1.12}$$

where L_{eff} is the effective length defined as $L_{eff} = [1-\exp(-\alpha z)]/\alpha$. The nonlinear time dependence of the phase of the field induces a variation of the instantaneous frequency commonly referred as the frequency chirp：

$$\Delta\omega(t) = -\frac{\partial\phi_{NL}}{\partial t} = -\left(\frac{L_{eff}}{L_{NL}}\right)\frac{\partial}{\partial t}|U(0,t)|^2 \tag{2.1.13}$$

It indicates that additional frequency components are generated in the pulse spectrum as the pulse propagates in the optical fiber, which will cause the spectrum broadening. This broadening is usually accompanied by the presence of an oscillatory structure in the optical spectrum resulting from the interference between two different parts of the pulse having the same instantaneous frequency. The chirp which is induced by the SPM will affect the pulse shape through the GVD. In the anomalous dispersion regime, the cooperation of them can make the pulse propagate as an optical soliton.

2.1.2 Cross-Phase Modulation (XPM)

When two or more optical fields having different wavelengths propagate simultaneously

inside an optical fiber, they will also interact with each other through the fiber nonlinearity. In general, such an interaction can generate new waves under appropriate conditions through a variety of nonlinear phenomena such as XPM, FWM, SRS and SBS. In the case of XPM, it is the phase change of an optical field induced by the nonlinear interaction with another optical field which may have a different wavelength, direction, or polarization state in the nonlinear Kerr medium. For fields with two different wavelengths, this can be described by noting that the total field is given by [17, Chapter 7.1] :

$$E = \frac{1}{2}\hat{x}\left[E_1 e^{-i\omega_1 t} + E_2 e^{-i\omega_2 t} + c.c.\right] \tag{2.1.14}$$

and the nonlinear phase shift for E_1 is :

$$\phi_{NL}(z) = n_2 \frac{\omega_1}{c} z\left(\left|E_1\right|^2 + 2\left|E_2\right|^2\right) \tag{2.1.15}$$

The first term is responsible for SPM and the second term results from the phase modulation of one light by another coupled light and is thus responsible for XPM. The factor of 2 in front of the second term indicates that XPM is twice as effective as SPM for the same intensity.

Both of the SPM-induced and XPM-induced chirps can be used to compress optical pulses. However, in contrast to the SPM case which requires the input pulse to be intense and energetic, the XPM can compress weak input pulses due to the fact that the frequency chirp is produced by a copropagating intense pulse.

2.1.3 Four-Wave Mixing (FWM)

The FWM is a nonlinear process related to the recombination of photons with different energies. It stems from the nonlinear interaction of four photons through the third-order susceptibility $\chi^{(3)}$ [19]. In the process of FWM, two photons at frequencies ω_1 and ω_2 are annihilated and then generate two new photons at frequencies ω_3 and ω_4 :

$$\omega_1 + \omega_2 = \omega_3 + \omega_4 \tag{2.1.16}$$

For the process to be efficient, the following phase-matching condition (which also means the conservation of momentum) should be satisfied :

$$\Delta k = k_1 + k_2 - k_3 - k_4 = 0 \tag{2.1.17}$$

A special case known as partially degenerate FWM occurs when $\omega_1 = \omega_2$, which indicates that the two photons of the single pump are annihilated to create two new photons, and which commonly referred the as Stoke and anti-Stoke photons in analogy with the SRS. This case is of practical interest because if an intense pump wave propagates along the fiber, the Stokes and anti-Stokes waves at the frequency ω_3 and ω_4 under the phase-matching condition described above can be built up from noise and are amplified through the FWM. We can also describe the FWM phenomena by considering the third-order polarization which is given by [17, Chapter 10.1] :

$$P_{NL} = \varepsilon_0 \chi^{(3)} \vdots EEE \tag{2.1.17}$$

and considering the four optical waves at frequencies ω_1, ω_2, ω_3, and ω_4 with linear polarizations along the same direction of axis x. The expression for P_{NL} can be described by :

$$P_{NL} = \frac{1}{2}\hat{x}\sum_{j=1}^{4} P_j \exp\left[i\left(k_j z - \omega_j t\right)\right] + c.c. \quad (2.1.18)$$

where P_j consists of a large number of terms involving the products of three electric fields. In the case of P_4, it can be described by：

$$P_4 = \frac{3\varepsilon_0}{4}\chi^{(3)}_{xxxx}\left[\left|E_4\right|^2 E_4 + 2\left(\left|E_1\right|^2 + \left|E_2\right|^2 + \left|E_3\right|^2\right)E_4 + 2E_1E_2E_3e^{i\theta_+} + 2E_1E_2E_3^*e^{i\theta_-} + \ldots\right] \quad (2.1.19)$$

$$\theta^+ = \left(k_1 + k_2 + k_3 - k_4\right)z - \left(\omega_1 + \omega_2 + \omega_3 - \omega_4\right)t \quad (2.1.20)$$

$$\theta^- = \left(k_1 + k_2 - k_3 - k_4\right)z - \left(\omega_1 + \omega_2 - \omega_3 - \omega_4\right)t \quad (2.1.21)$$

The first four terms containing E_4 in equation (2.1.19) are responsible for the SPM and XPM effects while others are responsible for the FWM. The effects of these phenomena in producing parametric coupling depend on the phase mismatch between E_4 and P_4, which is governed by θ^+ and θ^-, or a similar quantity.

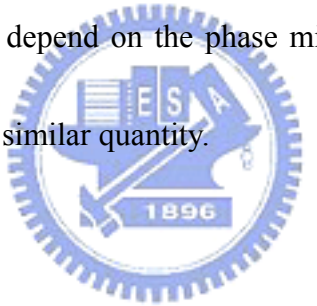

2.1.4 Stimulated Raman Scattering (SRS)

The process of the Raman effects is a kind of scattering phenomena which can transfer a small fraction of power from one optical field to another with the frequency downshifted by the amount determined by the vibration modes of the medium. These generated photons are commonly referred as the Stokes waves [20, Chapter 10]. In order to preserve the energy and momentum in the interaction, frequency-upshifted photons are also emitted and these new photons are referred as the anti-Stokes waves. The SRS has found applications in optical amplification and optical spectroscopy. It has a delayed response characteristics due to the

vibration contribution. For intense pump fields, the spontaneously emitted photons can further stimulate the emission of Stokes and anti-Stokes photons. The stimulated Raman scattering (SRS) consequently results in gain, which can be used to amplify a probe wave copropagating with the pump wave under the condition that its wavelength is located within the Raman gain bandwidth generated by the pump wave will be amplified through SRS. Actually, spontaneous Raman noise can act itself as a probe for the SRS.

The Raman gain spectrum is the most important quantity for describing the SRS, and it is related to the following equation [17, Chapter 8.1] :

$$\frac{dI_s}{dz} = g_R(\Omega) I_p I_s \tag{2.1.22}$$

where I_p represents the pump intensity, I_s represents the Stokes wave intensity, and $g_R(\Omega)$ is the Raman gain coefficient where Ω represents the frequency difference between the pump and the Stokes waves. It has been measured for silica fibers in experiments and in general, it depends on the composition of the optical fiber core and can vary significantly with the use of different dopant. The Raman gain bandwidth is very wide so that it is particularly important amplifying for large bandwidth signals which are very narrow pulses in the time domain.

Another thing we need to pay attention is the Raman threshold. Usually, the SRS is observed by using high-power lasers. For single mode fiber (SMF) with a typical effective area of 10 μm^2, the critical pump power is about 10 W for a 10 m optical fiber. At such power levels, the SRS can be observed with optical fibers only a few meters long.

2.1.5 Stimulated Brillouin Scattering (SBS)

The stimulated Brillouin scattering occurs when the light in a medium interacts with density variations and changes its path [20, Chapter 9]. Compared with the SRS, it requires much lower input power levels. The process of SBS will generates an acoustic wave and this wave in turn modulates the refractive index of the medium. From a quantum point of view, the process can be considered as one kind of light photon interaction with acoustic or vibrational phonons. It is similar to the SRS in the sense that it manifests through the generation of Stokes waves which frequency is downshifted from that of the incident light by an amount set by the nonlinear medium. However, in the case of SRS, the Stoke wave can be generated in not only the forward direction but also in the backward direction, while it can only be emitted in the backward direction in the case of SBS. In addition, the Stoke shift is smaller by three orders of magnitude for the SBS compared with the SRS.

The following equation can be used to describe the process of SBS [17, Chapter 9.1] :

$$\Omega_B = \omega_p - \omega_s \tag{2.1.23}$$

$$k_A = k_p - k_s \tag{2.1.24}$$

where ω_p and ω_s represent frequencies, and k_p and k_s represent the wave vectors, the suffix p and s mean the pump and Stokes waves, respectively. The frequency Ω_B and the wave vector k_A of the acoustic wave satisfy the standard dispersion relation :

$$\Omega_B = \nu_A |k_A| \approx 2\nu_A |k_p| \sin\frac{\theta}{2} \tag{2.1.25}$$

where θ is the angle between the pump and Stokes fields, and we set $|k_p| \approx |k_s|$. We can notice that the frequency shift of the Stokes wave is related to the scattering angle. Especially, Ω_B will be maximum and vanish in the backward and forward directions respectively. Therefore, SBS occurs only in the backward direction with the Brillouin shift given by：

$$\nu_B = \frac{\Omega_B}{2\pi} = \frac{2n\nu_A}{\lambda_p} \tag{2.1.26}$$

where n is the modal index at the pump wavelength λ_p, and we set $|k_p| = \frac{2\pi n}{\lambda_p}$. This equation indicates that SBS should occur only in the backward direction. However, because of the guided nature of acoustic waves which leads to the relaxation of the wave vector selection rule, spontaneous Brillouin scattering can occur in forward direction. Therefore, a small amount of Stokes light is generated in the forward direction, and it is referred to as guided-acoustic-wave Brillouin scattering.

2.2 Principles of optical amplifiers

The peak intensity of the input pulses will strongly affect the output supercontinuum bandwidth. Therefore, we will use a high power optical fiber amplifier for power amplification and pulse compression simultaneously. We use the cladding pumped fiber which is a special kind of multi-mode fiber (MMF) for the pump lights. It allows us to pump with a higher power so that the self-phase modulation and dispersion in the optical fibers can be exploited. The signal is guided in the central core region while the pump is guided by the

inner cladding. In addition, doping is confined to the center of the optical fiber core to amplify the signal mode, and to reduce the amplified spontaneous emission [21].

2.3 Principles of mode-locked fiber lasers

Mode-locking is a method to generate pulses trains by coupling and locking the phases of the cavity modes to each other. In a laser cavity, the total optical field can be written as [22]：

$$E(t)=\sum_{m=-M}^{M}E_m\exp(i\phi_m-i\omega_m t) \tag{2.3.1}$$

where E_m,ϕ_m, and ω_m are the amplitude, phase, and frequency of the modes respectively. These frequencies are separated by the mode spacing $\Delta\nu=c/2nL$. If all modes operate independently of each other with no definite phase relationship among them, the interference terms in the total intensity $|E(t)|^2$ average to zero, and this is the situation in multimode CW lasers. When the phases of these components are locked together, this laser modes act as a single coherent source and we can apply the fourier transform to see that the laser will generate a periodic pulse train. In the situation, assuming the amplitudes of the modes are equal, the total intensity becomes

$$|E(t)|^2=\frac{\sin^2[(2M+1)\pi\Delta\nu t+\phi/2]}{\sin^2(\pi\Delta\nu t+\phi/2)}E_0^2 \tag{2.3.2}$$

where ϕ is the phase difference between two neighboring modes. Experimentally this can be achieved by a variety of methods including the active and passive mode-locking. Typically,

the active mode-locking can easily get high repetition rate pulse trains, but the pulse-width is not very short so that the peak power is lower. On the other hand, the passive mode-locked laser can easily generate short pulse train in the sub-picosecond region, but it exhibits a low repetition rate.

2.3.1 Active mode-locked fiber lasers

The active mode-locking means that we use an electric signal to drive a modulator which can affect the light in the laser cavity to achieve the purpose of mode-locking. Usually we can use an amplitude modulator (AM) or a phase modulator (PM) as the active mode-locking component.

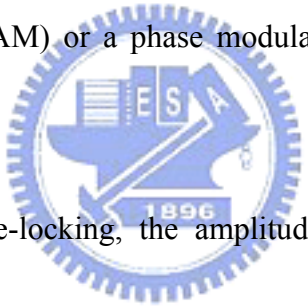

In the case of AM mode-locking, the amplitude of the light in the laser cavity is modulated directly by the AM modulator. It offers the periodic loss in the time domain so that only the pulses that pass through the modulator at the lowest loss will exist. Each time the pulses pass through the modulator, the pulse-width becomes shorter. However, shorter pulses experience larger dispersion when propagating inside the cavity. When the two forces are balanced, we can get the steady state pulse shape.

In the PM mode-locking case, the PM offers a change of the phase instead of the amplitude for shortening the optical pulse through the combination effects of dispersion. Again, the shorter pulses experience larger dispersion effects and we get the stable pulse

shape when the two forces balance to each other.

On the experimental side, the typical active harmonic mode-locked lasers always require additional components in the laser cavity to solve the noise problems. We can add a Fabry-Perot filter in the laser cavity, and by adjusting the free space distance, the free spectral range of the etalon can be matched to the cavity harmonic frequency. In this situation, there will be only one supermode that will survive so that the supermode noise can be suppressed. The second method is to use an optical band-pass filter. By cooperating with the SPM, the pulse amplitude is clipped to a certain intensity level with a stable pulse energy. Another method is to make use of a semiconductor optical amplifier (SOA) [23] which acts as a fast saturable absorber to reduce the laser intensity noises. In addition, we can change the laser structure to utilize the regenerative mode-locking which is accomplished through a feed-back system using the self-beating signal of the output pulses. The phase between the pulse train in the cavity and the modulation signal is automatically adjusted so that the pulses will always experience maximum transmission when they propagate through the modulator. Also, we can use the additive-pulse limiting (APL) which employs the concept of additive-pulse mode-locking (APM) by using the nonlinear polarization rotation effect with a different bias point to suppress the pulse-to-pulse amplitude fluctuations in a harmonic mode-locked fiber laser.

2.3.2 Passive mode-locked fiber lasers

Passive mode-locked lasers can generate ultra-short pulse trains by making use of nonlinear effects only [24]. This kind of lasers does not utilize any active component such as a modulator but uses the intensity dependent optical devices to provide the self-induced modulation effects. Several methods will be introduced in the following.

The first method is to make use of a fast saturable absorber whose absorption can change on the timescale of the pulse-width. The equation of the loss modulation caused by the fast saturable absorber can be expressed as in the following：

$$s(t) = \frac{s_0}{1 + I(t)/I_{sat}} \tag{2.3.3}$$

where s_0 is the unsaturated loss, $I(t)$ is the light intensity, and I_{sat} is the saturation intensity of the absorber. When the optical pulse in the laser cavity passes through the absorber, its wings experience much more loss than the central part which is intense enough to saturate the absorber. In this way, this effect will shorten the pulse.

The additive-pulse mode-locking (APM) is the second technique for passive mode-locking. The concept is to utilize a nonlinear interferometer composed of two coupled cavities which contains a gain medium in one cavity and a Kerr medium in another to generate shorten pulses [25]. We can imagine that it works as an intracavity interferometer with a nonlinear phase modulator caused by the Kerr effect.

$$n = n_0 + n_2 I \tag{2.3.4}$$

where n_2 is the nonlinear index of refraction. The net nonlinear phase shift is

$$\phi = n_0 k_0 z + n_2 I k_0 z \tag{2.3.5}$$

where $n_2 I k_0 z$ is the nonlinear phase shift, and it is obviously that the magnitudes of the phase shifts for the peak and the wings of the pulse are different because of different intensities. If the lengths of the two cavities are adjusted appropriately to make the central part of the pulse experiences constructed interference and the wings of the pulse experience destructed interference, then the central part of the pulse will have less loss and thus the mode-locking can be achieved.

The third method is the polarization rotation additive-pulse mode-locking (P-APM). It use only one cavity to achieve the APM mode-locking. When the initial polarization state is elliptical in an optical fiber, the nonlinear polarization rotation effect can occur. We can use two polarization controllers and one polarization dependent isolator (which is equivalent to a polarization independent isolator and a polarizer) to demonstrate the P-APM. The first polarization controller and polarizer transform the linear polarization into the elliptic polarization, which can be viewed as the combination of the right-hand and left-hand circular polarization components. These components will accumulate different nonlinear phase shifts depending on their intensities. If the axis of the polarizer is set appropriately, the wings of the pulse will be attenuated and the pulse will be shorten.

The Kerr-lens mode-locking (KLM) is a method using the self-focusing to achieve

passive mode-locking. The size of the central part of the pulse will be smaller than that of the wings when the light propagates through a Kerr medium. It causes the center of the pulse to interact with the pumping light with higher intensity and the wings to interact with the pumping light with lower intensity. Eventually, the center of the pulse experiences a higher gain than the wings, and the pulse is shortened.

2.3.3 Hybrid mode-locked fiber lasers

The technique that combines more than one kind of mode-locking mechanisms in the same laser cavity to improve the performance is called the hybrid mode-locking [26]. The basic type of hybrid mode-locked fiber lasers is to add an amplitude modulator or a phase modulator into a passive mode-locked fiber laser. The modulator is used to generate high repetition rate pulses by offering periodic timing slots and the components of the passive mode-locked fiber laser are used to shorten the pulse-width efficiently. Using this technique, we can produce a pulse train with the higher repetition rate that can not be expected from passive mode-locked fiber lasers and the shorter pulse-width which is hardly generated from active mode-locked lasers. In addition, we can demonstrate an alternative hybrid mode-locking laser by adding a real slow saturable absorber in the laser cavity with a fast saturable absorber. The slow saturable absorber can provide several picosecond pulses for the fast saturable absorber to starting mode-locking.

2.3.4 Asynchronous mode-locked fiber lasers

In the previous sections, we mentioned that the mode-locked fiber laser using a modulator needed to be driven by an electric signal with frequency which is the same as on of the cavity harmonic frequencies. This is the so called synchronous mode-locked fiber lasers. As long as the anomalous group velocity dispersion (GVD) and SPM are intense enough, we can generate soliton-like pulse trains. It is obvious that the fluctuations of the cavity harmonic frequency, which may be caused by the variation of the cavity length (caused by the variation of environmental vibration, humidity and temperature), will strongly affect the stability of the mode-locked fiber laser.

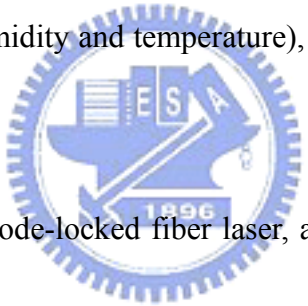

In order to stabilize the mode-locked fiber laser, an approach utilizing an asynchronous phase modulation (a phase modulator which is driven by an electric signal with the frequency different from the cavity harmonic frequency purposely) has been proposed, and the method is called the asynchronous mode-locking. The induced periodic frequency shift in asynchronous mode-locking will make noises in the cavity experience larger loss while the solitons can resist it and stay in good shape.

The main equation for mode-locked fiber laser using a phase modulator with the GVD and SPM effects can be expressed as [27]：

$$T_R \frac{\partial A}{\partial T} = \left\{ (g - l) + \left(\frac{g}{\Omega_g^2} + jD \right) \frac{d^2}{dt^2} + j\delta |A|^2 + jM \cos\left[\Omega_M t + \Omega_M \Delta T(T) \right] \right\} A \qquad (2.3.6)$$

where T_R is the roundtrip time of the light propagating in the fiber ring cavity, g is the saturated gain per roundtrip, l is the loss, Ω_g is the gain bandwidth of the gain medium, D is the group velocity dispersion parameter, δ is the Kerr coefficient, M is the depth of phase modulation , and Ω_M is the modulation frequency. Under synchronous modulation, the cosine function can be approximated by a parabolic function. The pulse shape of the solitons which propagate in the ring cavity can be expressed as：

$$A_{soliton} = A_0 \sec h\left(\frac{t}{\tau_s}\right) \tag{2.3.7}$$

For soltions, they suffer almost the same loss under synchronous and asynchronous modulation, so that the required net gain to compensate for the filtering loss in these two kind of operations are also the same and can be expressed as [27]：

$$(g-l)_{soliton} = \frac{2}{3}\frac{g}{\Omega_g^2 \tau_s^2} \tag{2.3.8}$$

On the other hand, consider the lowest order mode which has the lowest decay rate for the noise term, the required net gain is [27]：

$$(g-l)_{noise} = \mathrm{Re}\sqrt{\left(\frac{g}{\Omega_g^2} + jD\right) j\frac{M\Omega_M^2}{2}} \tag{2.3.9}$$

If the required gain is higher for the noise term than the soliton, the noise will decay. The following equation shows that the noise decay rate is much faster than the detuning rate $|\Delta f|$ so that the solitons can remain stable over the noises.

$$|\Delta f| << \frac{1}{T_R}\mathrm{Re}\sqrt{\left(\frac{g}{\Omega_g^2} + jD\right) j\frac{M\Omega_M^2}{2}} \tag{2.3.10}$$

The frequency deviation between the modulation frequency and the cavity harmonic frequency has limitation. If we operate it over the upper limit, the noise cleanup mechanism achieved through accumulated frequency shifts is diminished. In addition, the modulation must periodically cycle into synchronism, thereby refreshing the timing of the pulses. The lower limit of the detuning rate is required to enforce pulse timing. The width of the spectrum for soliton is proportional to the soliton energy. The loss rate due to filtering in turn is proportional to the spectral width and thus is proportional to the soliton energy. Therefore, an energy which is determined by the filtering loss without the need for additional stabilization is obtained for each soliton. However, there exist sinusoidal variation of the carrier frequency and the corresponding position shift in the time domain under the operation of asynchronous mode-locking, which can also be explained by the soliton perturbation theory.

Chapter 3 Experimental Setup and Results

3.1 1GHz ASM fiber laser

In our experiment, we use a ASM mode-locked fiber laser operated at the 1 GHz repetition rate as the first stage light source. The reason we do not use typical active or passive mode-locked fiber lasers is because of the difficulty of getting short pulse width and the high repetition rate simultaneously. In addition, the stability of the ASM fiber laser is much helpful for the proceeding of the experiment.

Two 980 nm laser diodes are used as the pumping source, and two WDM couplers are used to couple the 980 nm light into the ring cavity. In order to get more nonlinearity in the fiber cavity, high intracavity light intensity is needed. Therefore, the method of bi-directional pumping is utilized in the experimental setup.

An optical tunable filter is used to select the lasing wavelength of the laser. It can also suppress the supermodes and achieve a high SMSR by cooperating with the self-phase modulation (SPM) effect. Besides, the wide bandwidth of the bandpass filter can support shorter pulses in the cavity so that the generated pulse width also can be shorter.

The polarization controllers can change the polarization to adjust the APM. The phase modulator, which is the main component of typical active mode-locked fiber lasers, and the two polarization controllers also provide the mechanism of additive pulse mode-locking. If we replace the phase modulator with a polarization dependent isolator, the laser will become

typical passive mode-locked fiber laser.

Since the laser may be very sensitive to optical feedback which can strongly affect the performance of the laser under mode-locked operation, an isolator is used to make sure the pulses only propagate in one direction.

The output coupler is put behind the isolator and the coupling ratio is 30：70. This means that we keep 70% of the lights stay in the ring cavity and 30% of the lights to be the output pulses. Table 3.1 shows the components we use in our mode-locked fiber laser cavity, and figure 3.1 shows the experimental setup using these components.

Table 3.1 Components in the ring laser cavity

980nm pump laser：pump current at 300mA x 2
Erbium doped fiber：Low concentration, 6m
WDM Coupler x 2
Optical tunable filter：3 dB bandwidth is about 14 nm
Polarization controller：loops x 2
Phase modulator：from D.C. to 1 GHz
Isolator
Corning SMF：about 37m

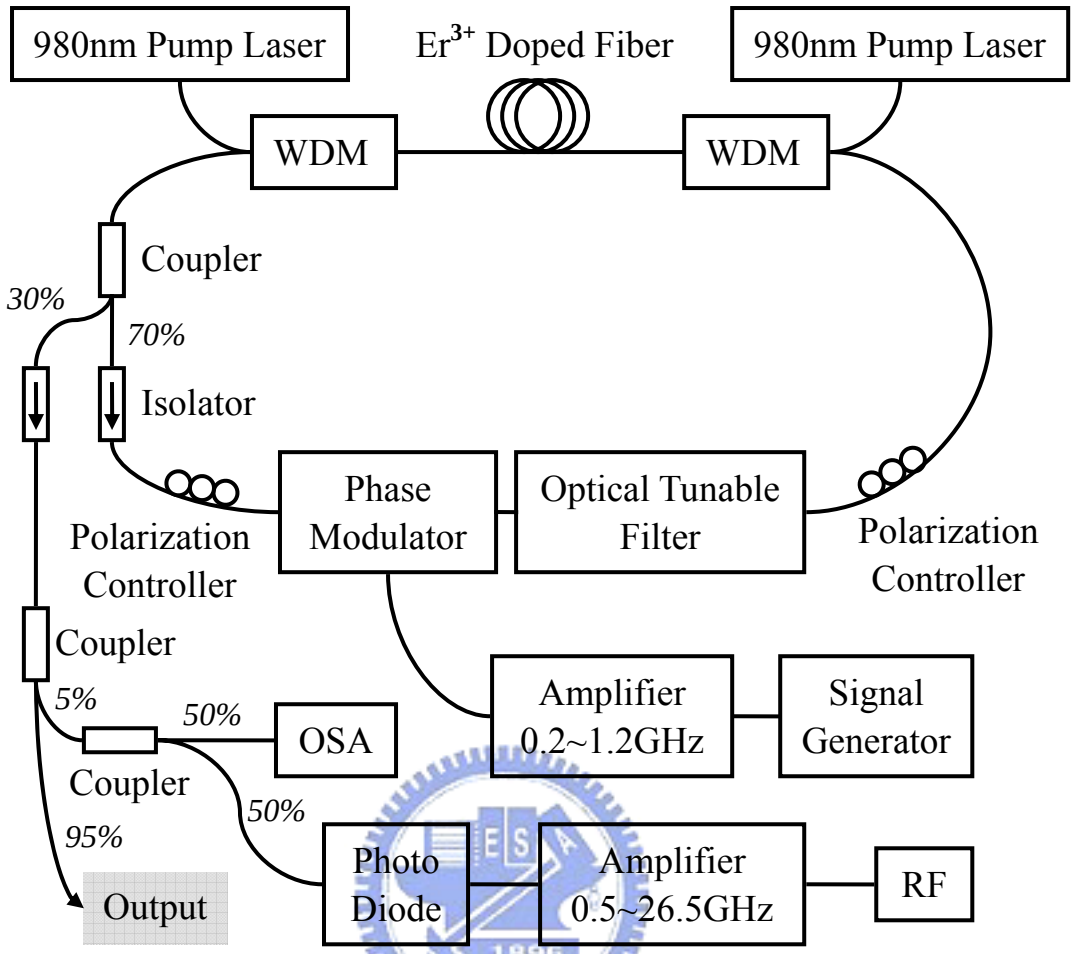

Fig 3.1 1 GHz ASM fiber laser experiment setup

For experimental operation, we first turn on the two 980nm pump laser, so that the Erbium fiber will amplify lights at 1550nm. After applying the RF, we observe that the output signal has lots of harmonic terms with the 4.2 MHz free spectral range. Since we want to operate the mode-locked fiber laser around 1GHz repetition rate, we choose the 238th harmonic term that will operate the mode-locked fiber laser with the repetition rate equal to 1.0021879 GHz. After determining the harmonic term, we set signal generator to the chosen repetition rate. At this state, we observe that the optical spectral bandwidth is about 0.72 nm

and this is the so called active mode locking or synchronous mode locking. Than we set the modulation frequency different from the 238th harmonic term about 8 kHz. It is obviously that the optical spectral bandwidth is broader than synchronous mode-locking. However, the supermodes suppression ratio (SMSR) is very terrible, so that we should adjust the polarization controllers and the optical filter to change the polarization and central wavelength to suppress supermodes. In order to getting a higher SMSR, we set the RF spectrum analyzer with 100 kHz span and adjust the two polarization controllers and the optical filter to balance the beating terms around the 238th harmonic frequency. More balanced the beating terms are, more chance the stable mode-locking operation with a high SMSR you can get. At 1 GHz, the ASM mode-locked fiber laser can usually be stabilized for half a day so that we can proceed the experiments without difficulties.

The optical spectral bandwidth of the output pulses we finally get is about 1.6 nm, centered at 1545.24 nm, as is shown in figure 3.2. The pulse width measured by an autocorrelator is about 1.8 picosecond, as shown in figure 3.3 with a Sech transform-limited time-bandwidth product of 0.36. The output power is about 14mW and the pumping power is about 340 mW. Figure 3.4 shows the RF spectrum and the SMSR is about 70dB. In figure 3.5, it shows the RF spectrum with 100 kHz span and we can observe that the deviation frequency is about 8 kHz. Figure 3.6 shows the RF spectrum with 3.5 GHz span. The lower SMSR in this figure is caused by the decreased resolution, and the noise distributed from 500 MHz to

3.5 GHz is caused by the amplifier with a bandwidth from 500 MHz to 26.5 GHz. The measured value signal located at 0 GHz is caused by the DC term, and the signals at 2 GHz and 3 GHz are laser harmonic components. The experimental parameters and results of the 1 GHz ASM fiber laser are list in Table 3.2. In addition, we can operate the laser at different central wavelength without changing the structure of the mode-locked laser by tuning the optical filter. Figure 3.7 and figure 3.8 indicate that the ASM fiber laser can also be operated at 1556.78 nm and 1535.08 nm.

Table 3.2 Experimental parameters and results of the 1GHz mode-locked fiber laser

Experimental parameters and results	
980nm pump laser	170 mW x 2
Cavity length	49.3 m
Free spectral range	4.2 MHz
Repetition rate	1.0021879 GHz
Modulation strength	25dBm
Optical spectral bandwidth	1.6nm
Central frequency	1545.24nm
SMSR	70dB
Frequency deviation	8 kHz
Output average power	14 mW
Output peak power	7.8 W
Pulse width (FWHM)	1.8 ps
Time-Bandwidth Product	0.36 (Sech fitting)

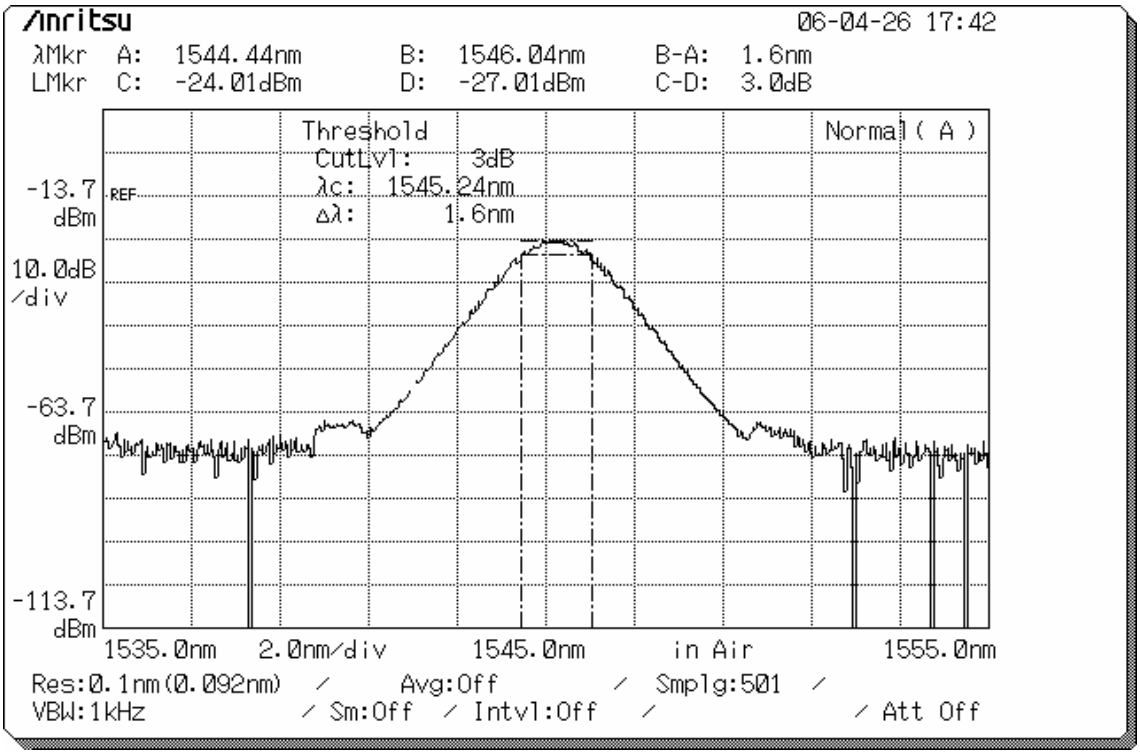

Fig 3.2 Optical spectrum for 1 GHz ASM fiber laser at 1545.24nm

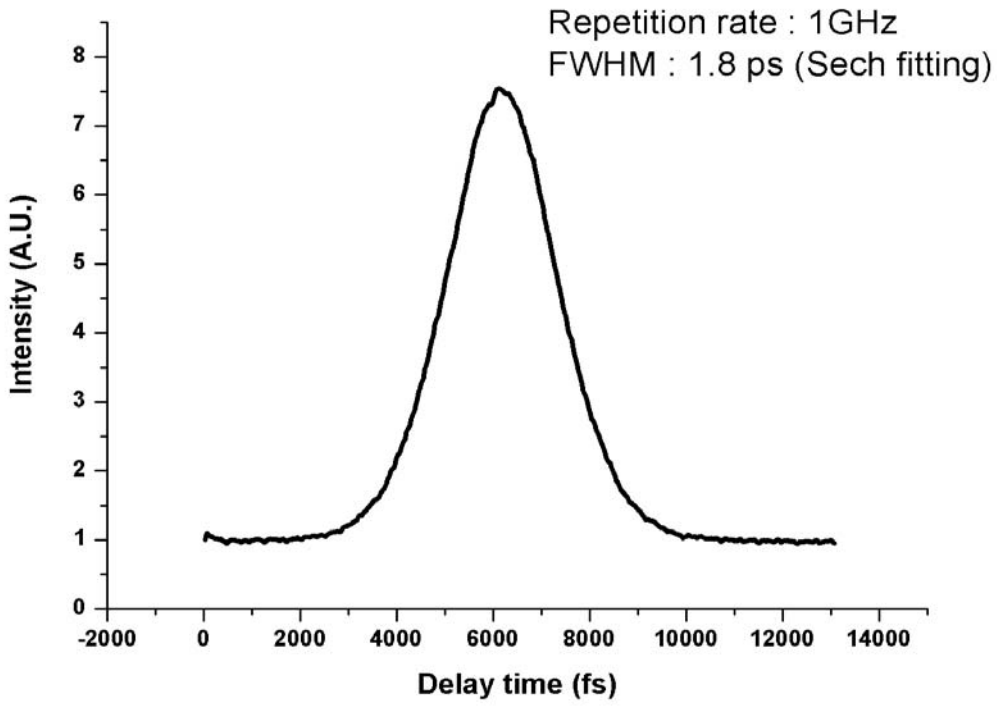

Fig 3.3 The autocorrelation of the pulse from 1 GHz ASM fiber laser

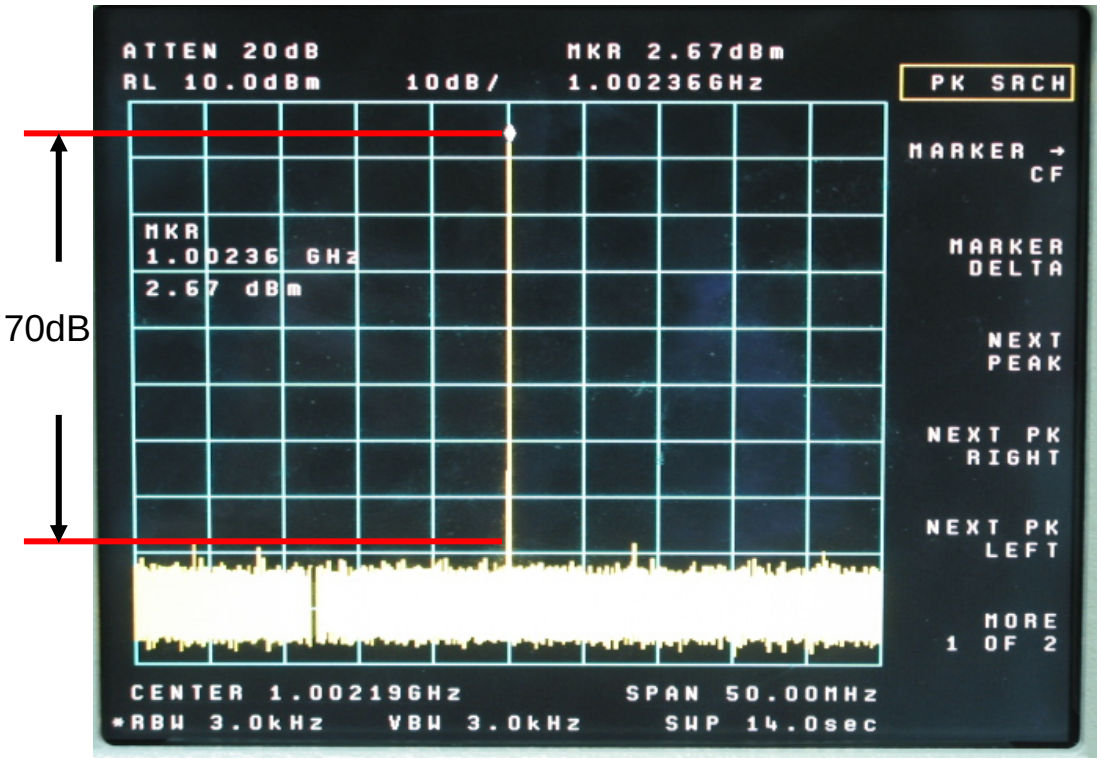

Fig 3.4 RF Spectrum span in 50 MHz

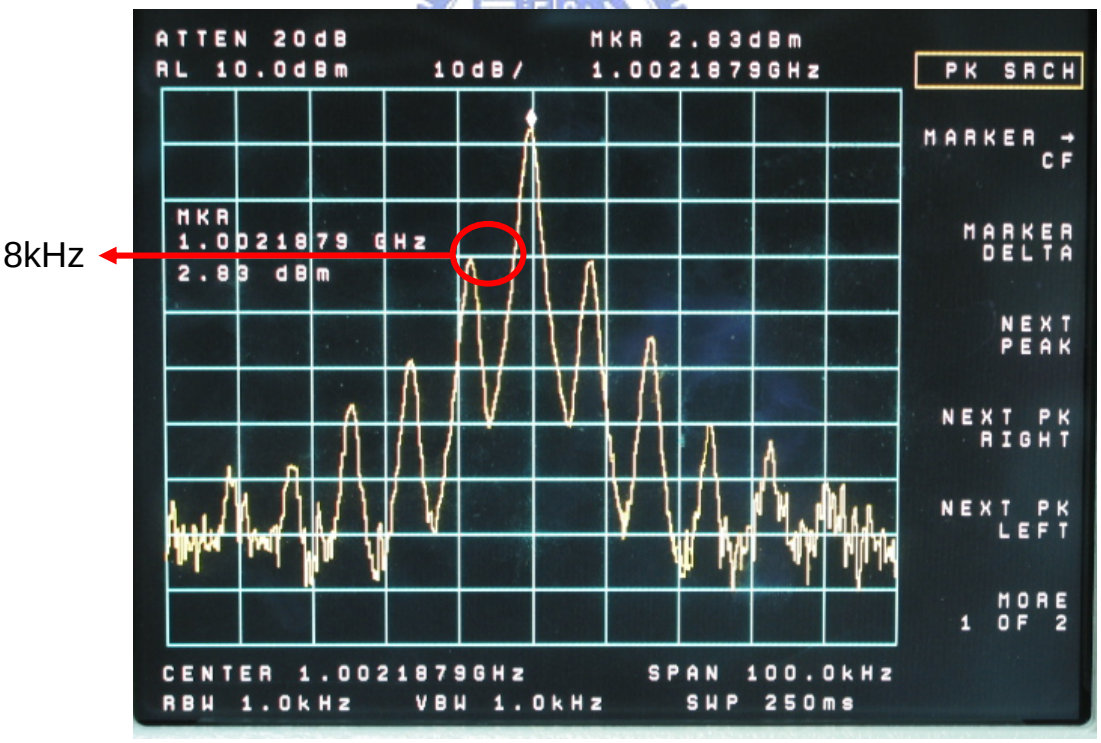

Fig 3.5 RF Spectrum span in 100 kHz

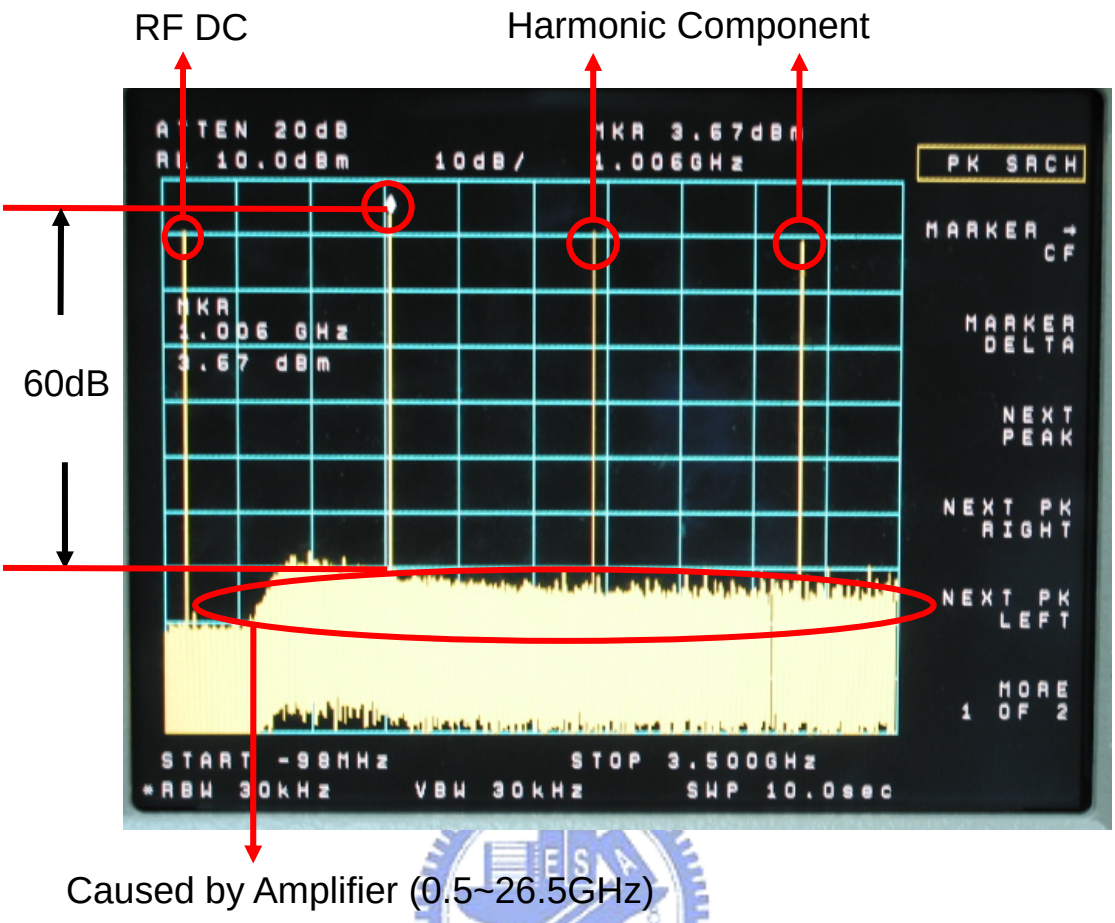

Fig 3.6 RF Spectrum span in 3.5 GHz

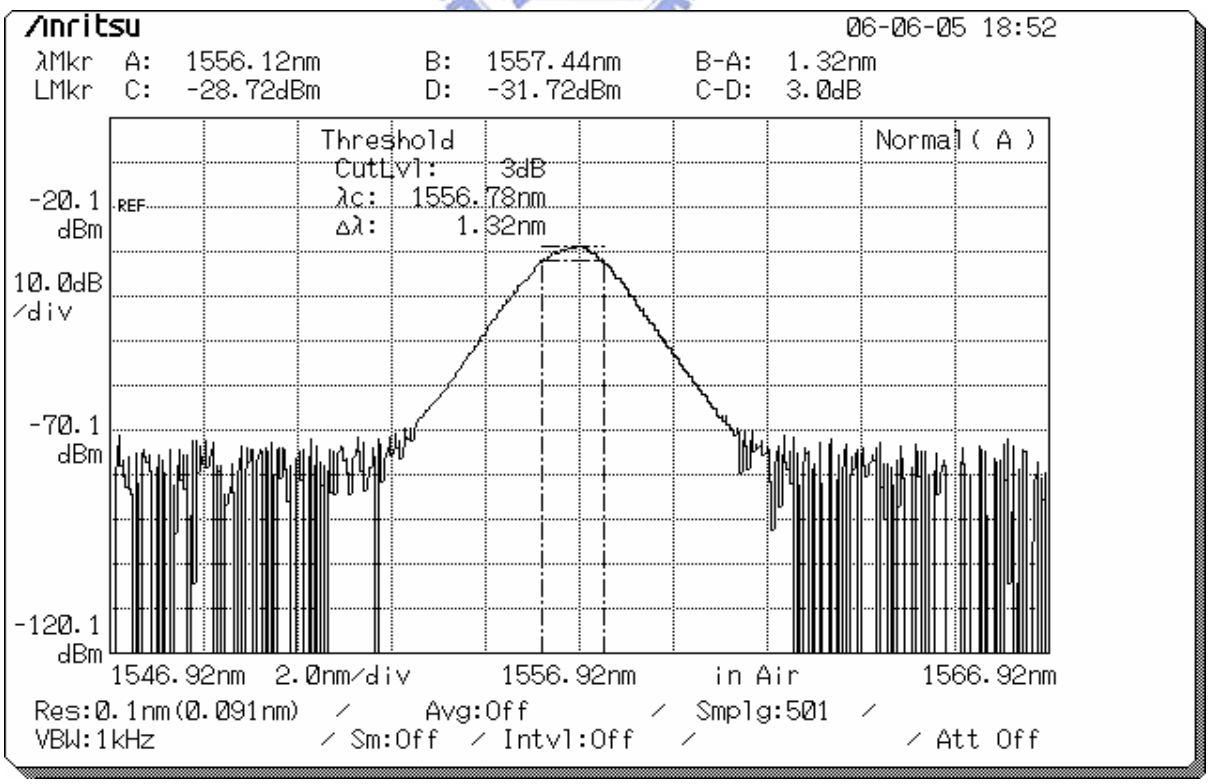

Fig 3.7 Optical spectrum for 1 GHz ASM fiber laser at 1556.78 nm

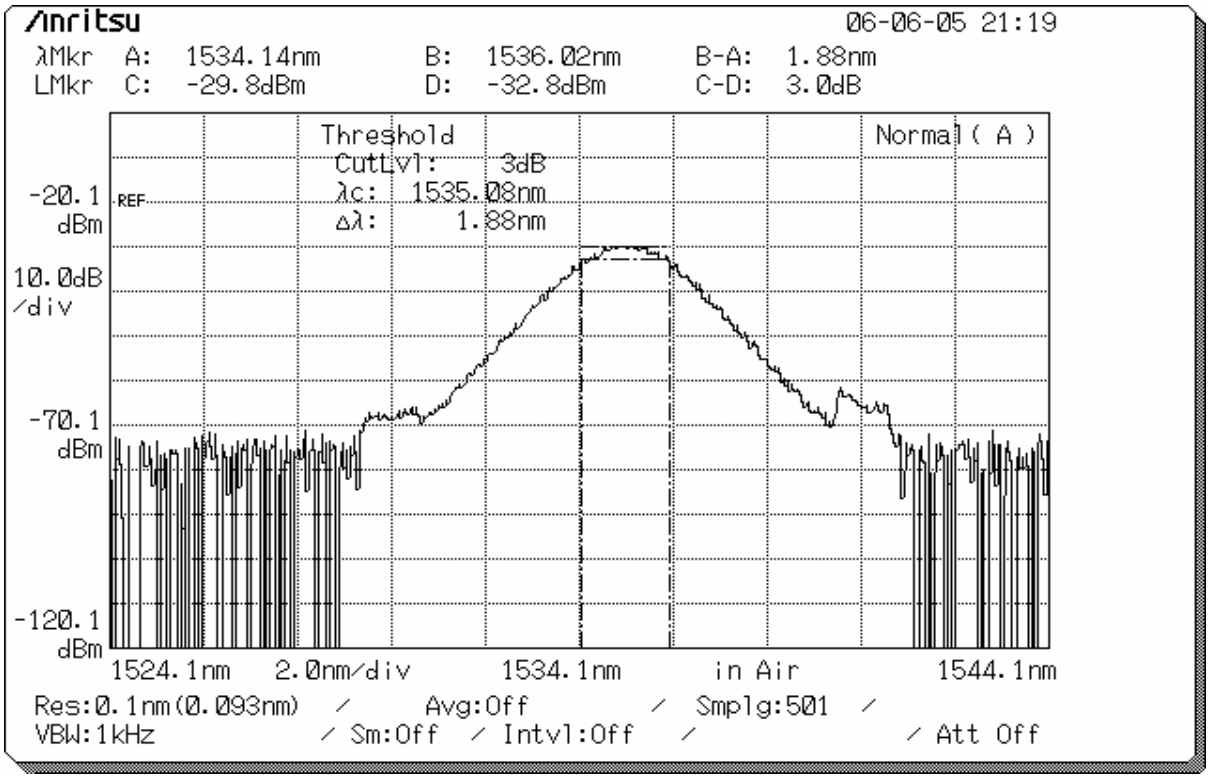

Fig 3.8 Optical spectrum for 1 GHz ASM fiber laser at 1535.08 nm

3.2 High power optical amplifier and HNLF for Supercontinuum generation

Since we have already established a stable short pulses light source, we then launched the pulse train into the optical Er-Yb fiber amplifier for raising the power. This will be helpful for the supercontimuum generation. Figure 3.9 shows the experimental setup. The fiber amplifier contains a power combiner and a section of 10m gain fiber (Er-Yb cladding pump fiber) from OFS, as shown in figure 3.10, and is pumped (forwardly) by a laser diode (6W) with a wavelength at 980 nm. Before the ASM mode-locked laser pulse is launched into the optical amplifier, we use a SMF to induce some chirp. The SPM due to n_2 in optical fibers is normally associated with the spectral broadening [28]. However, for a pulse whose chirp is initially negative the SPM actually causes the spectrum to compress [29][30]. In other words, the power from the wings of the spectrum is nonlinearly converted to the power at the central frequency, leading to the narrowing of the optical spectrum. We notice that the optical spectrum which is detected from the output of the optical amplifier is compressed after we add the SMF every time. The best value for the length of the pre-SMF in our measurement is 3.9 m, which is composed of an isolator and the input port of the power combiner. After the optical amplifier, the average power is raised from 14 mW, which is directly from the ASM fiber laser, to 1.2 W. However, the pulse width becomes 2.1 ps and it is broader than the input pulses. As mention before, we need the pulses with higher peak powers for obtaining stronger nonlinear effects in the HNLF. Hence, we add a section of SMF after the optical amplifier for

pulse compression. Figure 3.11 shows that the pulse width is related to the length of the SMF (for pulse compression). We finally choose the length of the SMF to be 25 m (this is in the case with input pulse width 2.0 ps) and the pulse width is compressed to 414 fs with the optical bandwidth about 65.6 nm. Figure 3.12 and Figure 3.13 shows the optical spectrum and the autocorrelation of the pulse after pulse compression. In figure 3.13, we can notice that the output pulse we get has some pedestals, and the pulse quality (the ratio of energy in the central pulse to the total pulse energy) is approximately 42%, corresponding to a peak power of 1.2 kW. After pulse compression, we launch the pulse train into the HNLF to generate supercontinuum light. In this work, we use two kinds of HNLF, and the specifications are shown in Table 3.3. First, we use HNLF-A with the length of 10 m, and the output spectrum is detected by an optical spectrum analyzer and the generated wavelengths span from 1260 nm to over 1800 nm as shown in Fig 3.14. In figure 3.15, it shows the optical spectrum of supercontinuum light by using 0.5 m HNLF-A. We can notice that the spectrum spans from about 1300 nm to 1740 nm and is obviously shorter than the previous result by using 10 m HNLF-A. In order to improving the performance, we use HNLF-B with different dispersion and nonlinearity and the length is about 0.95 m. Figure 3.16 shows the result and it is obviously that the optical spectrum spans broader which ranges from 1120 nm to over 1800 nm.

In the experiment, if we bend the SMF after the optical fiber amplifier, the shape of

supercontinuum spectrum will a little bit change. This is caused by the change of polarization and it result in different effective indices for the waves propagating with orthogonal polarizations. The index difference can be expressed as [17, Chapter 10.3] :

$$\delta n = \Delta n_x - \Delta n_y \tag{3.2.1}$$

where Δn_x and Δn_y represent changes in the refractive indices for the optical fields polarized along the slow and fast axes of the fiber, respectively. It will cause a variation of phase-matching and affect the shape of the output spectrum.

As mention before, since the pulse after pulse compression has some pedestal, we try to find out the reason so that we can improve it. First, we replace the ASM fiber laser with a typical passive mode-locked fiber laser which is operated at repetition rate 15 MHz. Figure 3.17 and figure 3.18 show the optical spectrum and autocorrelation trace of the passive mode-locked fiber laser. In figure 3.18, we notice that it is not a single pulse. After launching it into the fiber amplifier, we notice that there are greater pedestals for the output pulse as shown in figure 3.19. Then we operate the passive mode-locked fiber laser in the soliton bound-state mode, which means that there exist two pulses closely spaced. Figure 3.20 and figure 3.21 shows the optical spectrum and autocorrelation trace in this case. After launching the pulse train into the fiber amplifier, we notice that the pedestal is obviously smaller than the previous case as shown in figure 3.22. Therefore, we consider that the pulse train we use in this experiment may not be pure enough, and that is the part we are going to improve. In

addition, we also tried to change the pumping of the optical fiber amplifier from forward to backward. However, the result is almost the same as the forward case.

Figure 3.23 shows the optical spectrum of the supercontinuum light by using another optical spectrum analyzer (900 nm ~2600 nm). The optical bandwidth ranges from 1100 nm ~ 2300 nm.

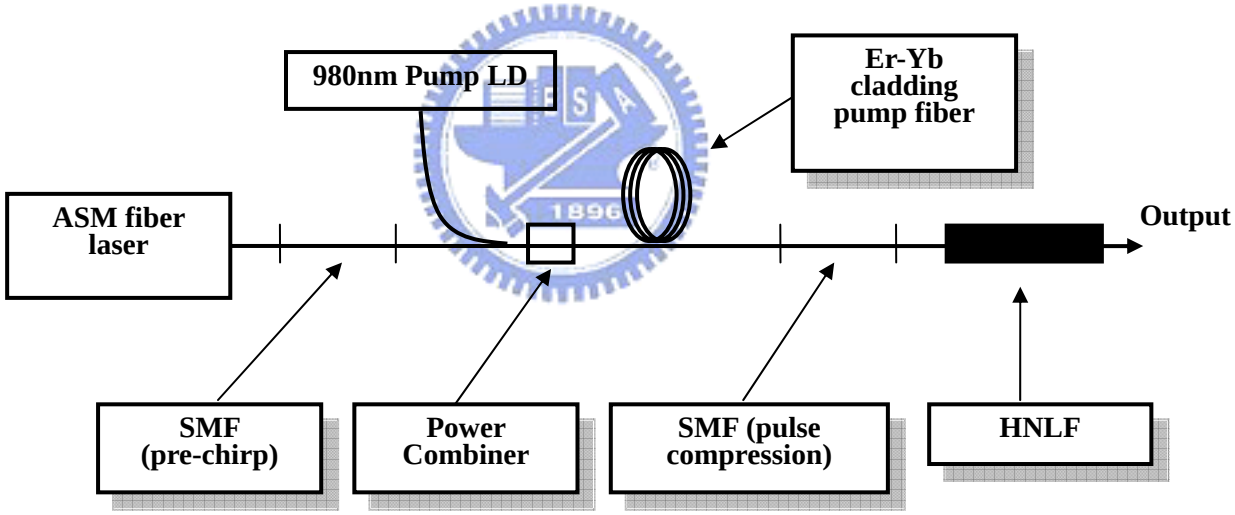

Fig. 3.9 Supercontinuum generation system setup

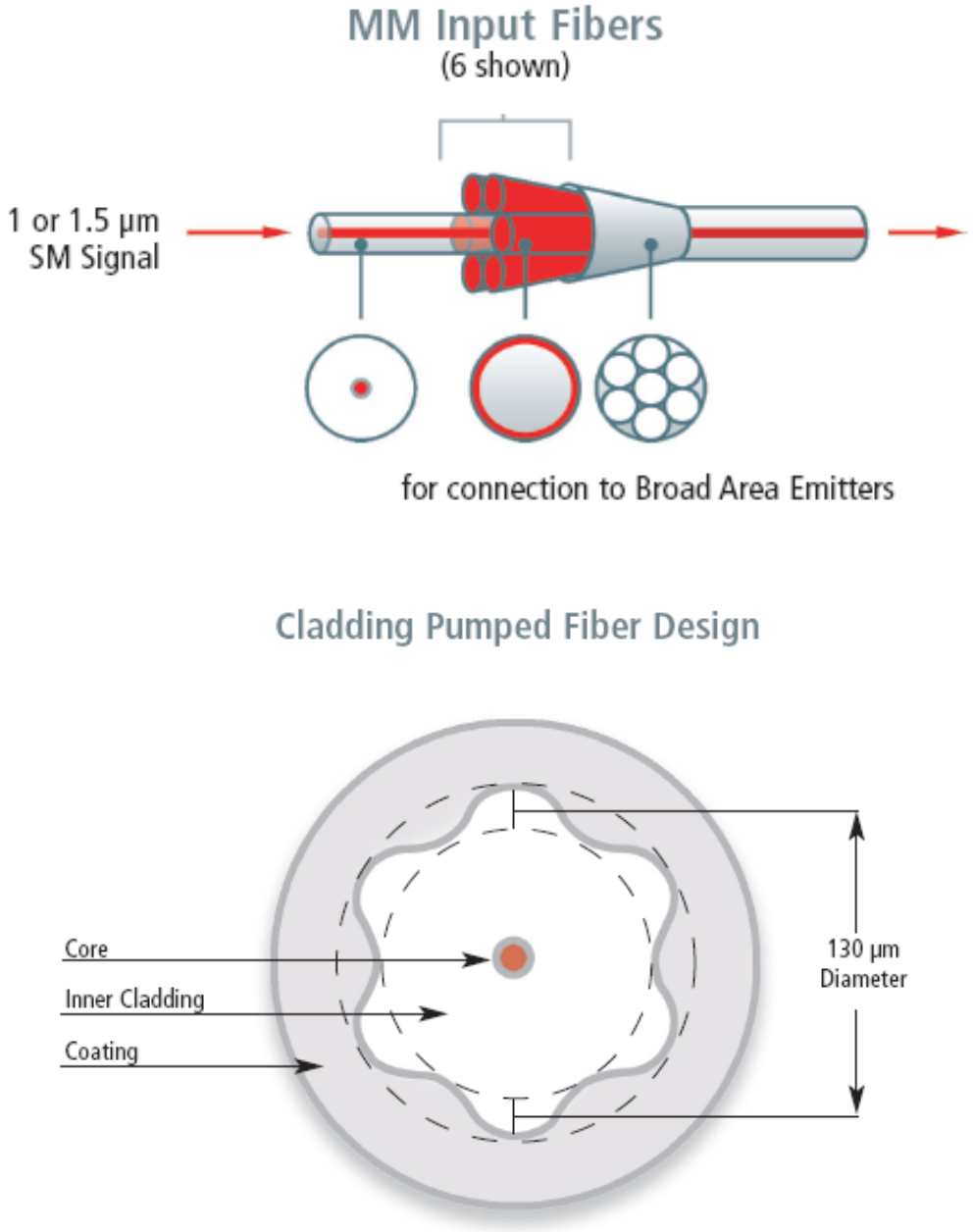

Fig 3.10 Structure of the optical fiber amplifier From OFS (http://www.specialtyphotonics.com)

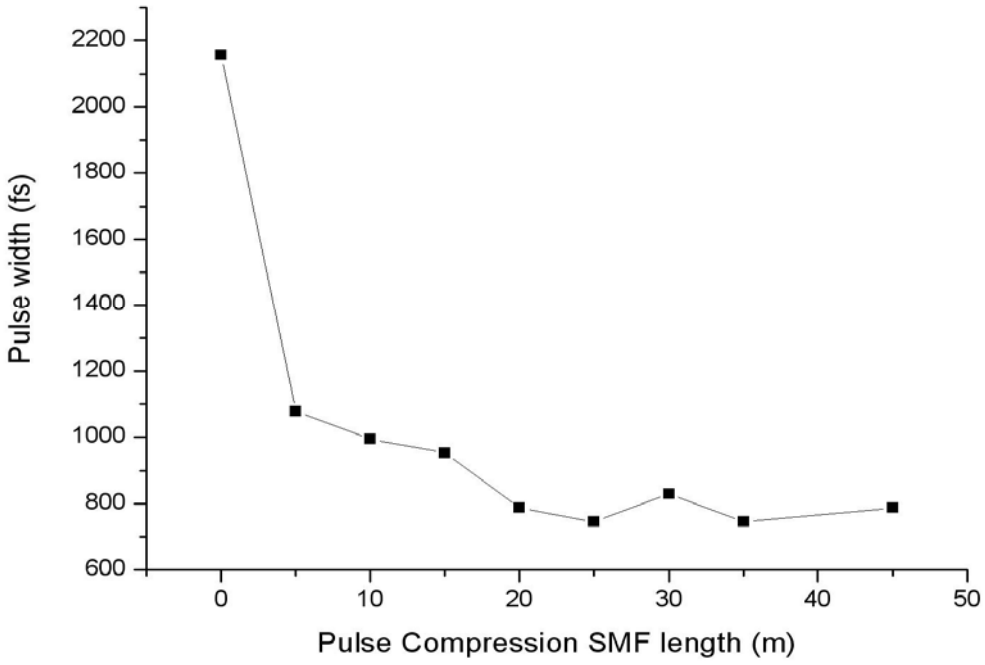

Fig 3.11 The pulse width after the optical amplifier vs. the length of the SMF (pulse compression)

Table 3.3 Specification of HNLF

	HNLF-A	**HNLF-B**
Dispersion (ps/nm/km)	-0.06~0.8	1.74
Dispersion Slope (ps/nm^2/km)	0.04	0.01
Nonlinearity (1/W/Km)	11.1	10.5

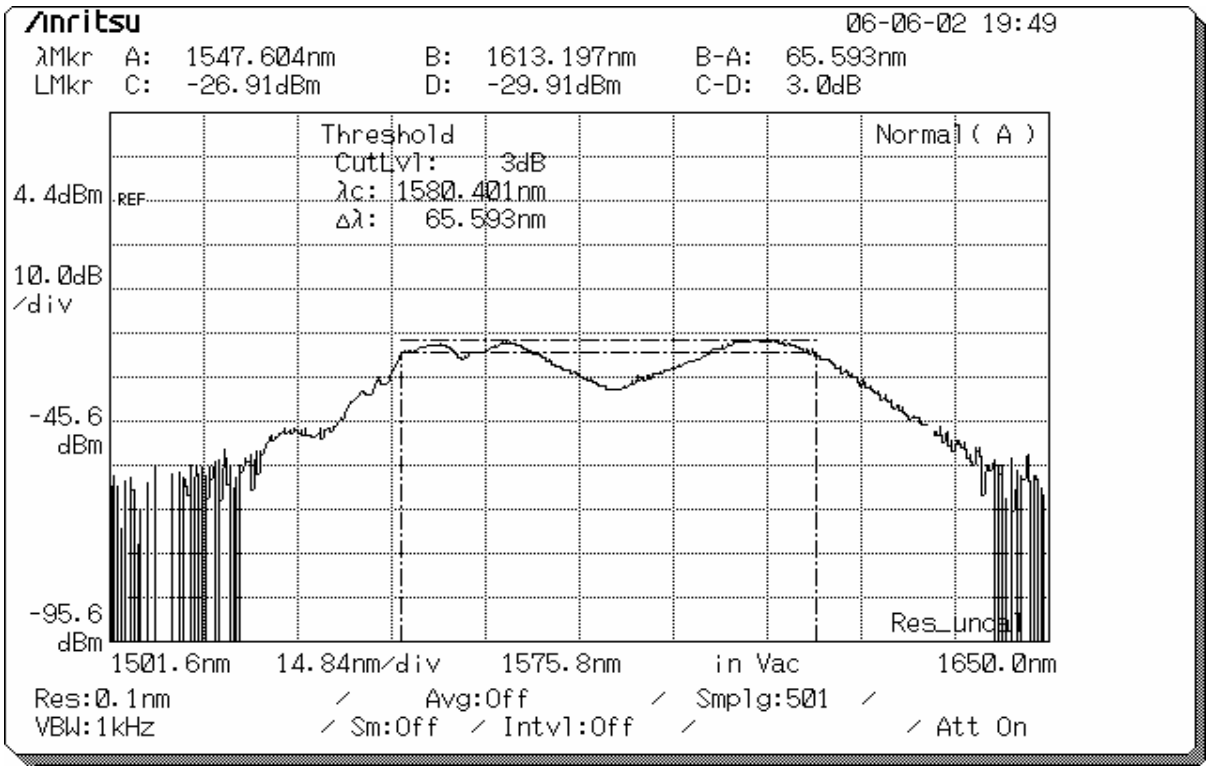

Fig 3.12 Optical spectrum of the compressed pulse

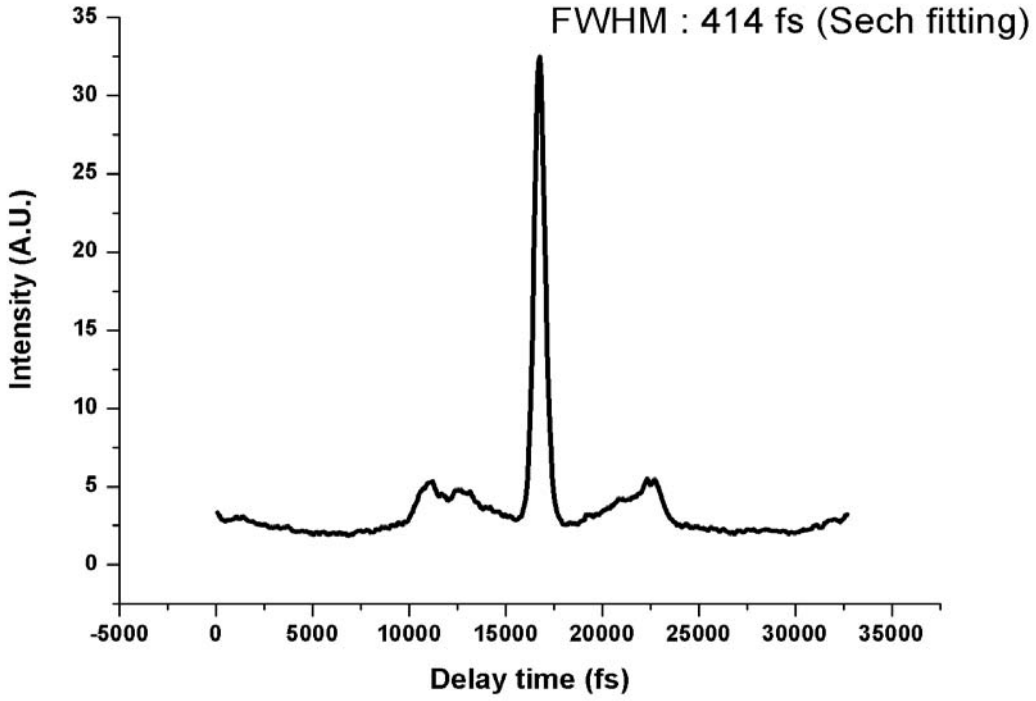

Fig 3.13 Autocorrelation of the compressed pulse

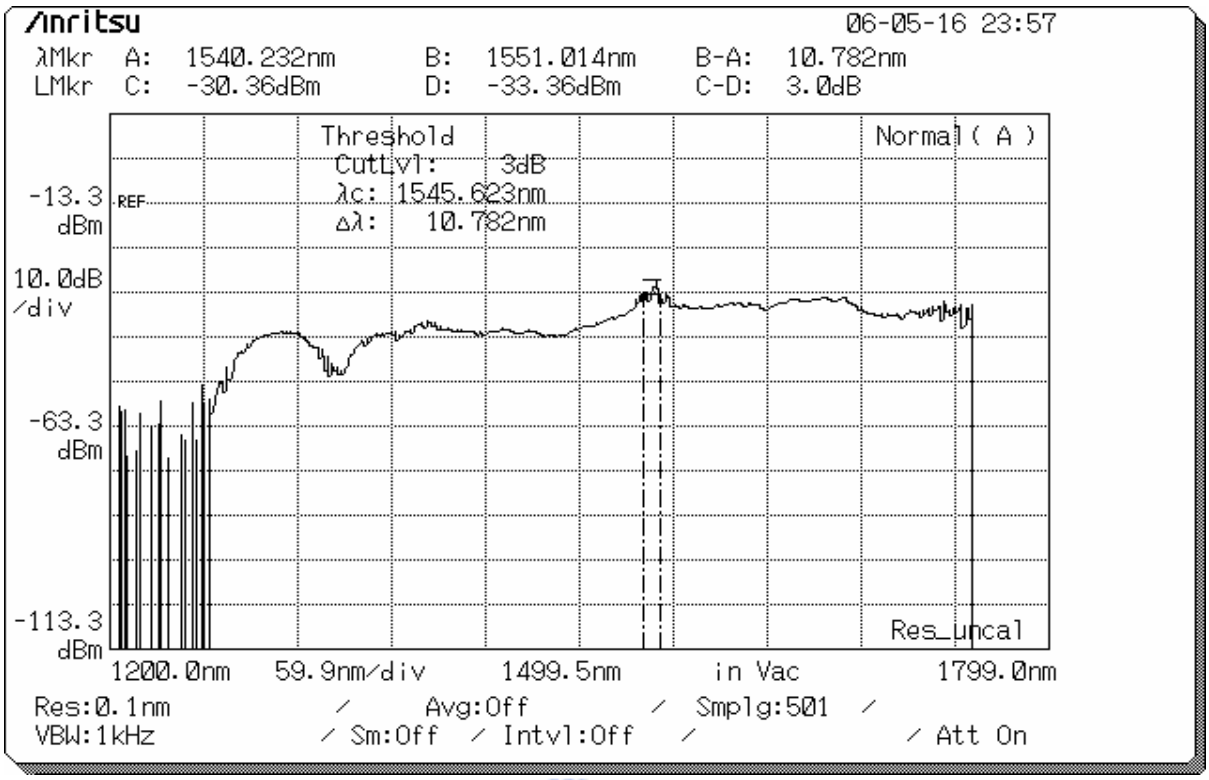

Fig 3.14 Optical spectrum of the Supercontinuum using 10 m HNLF-A

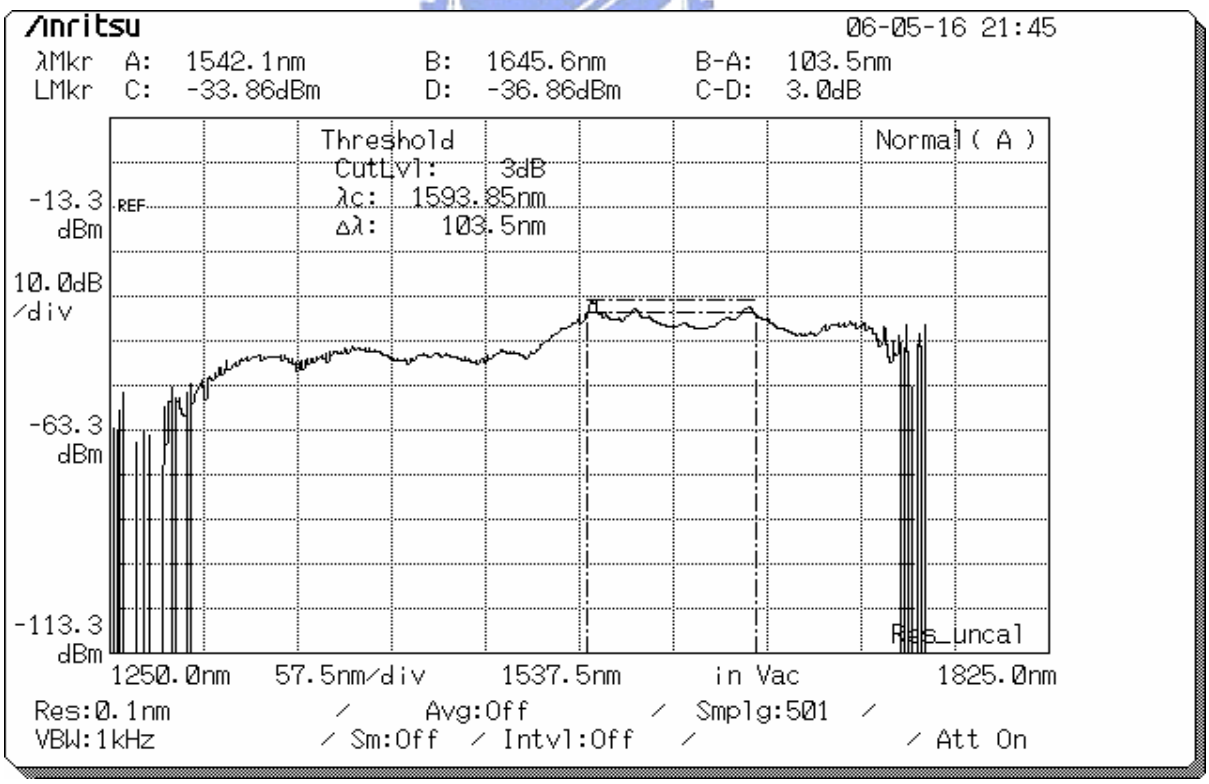

Fig 3.15 Optical spectrum of the Supercontinuum using 0.5 m HNLF-A

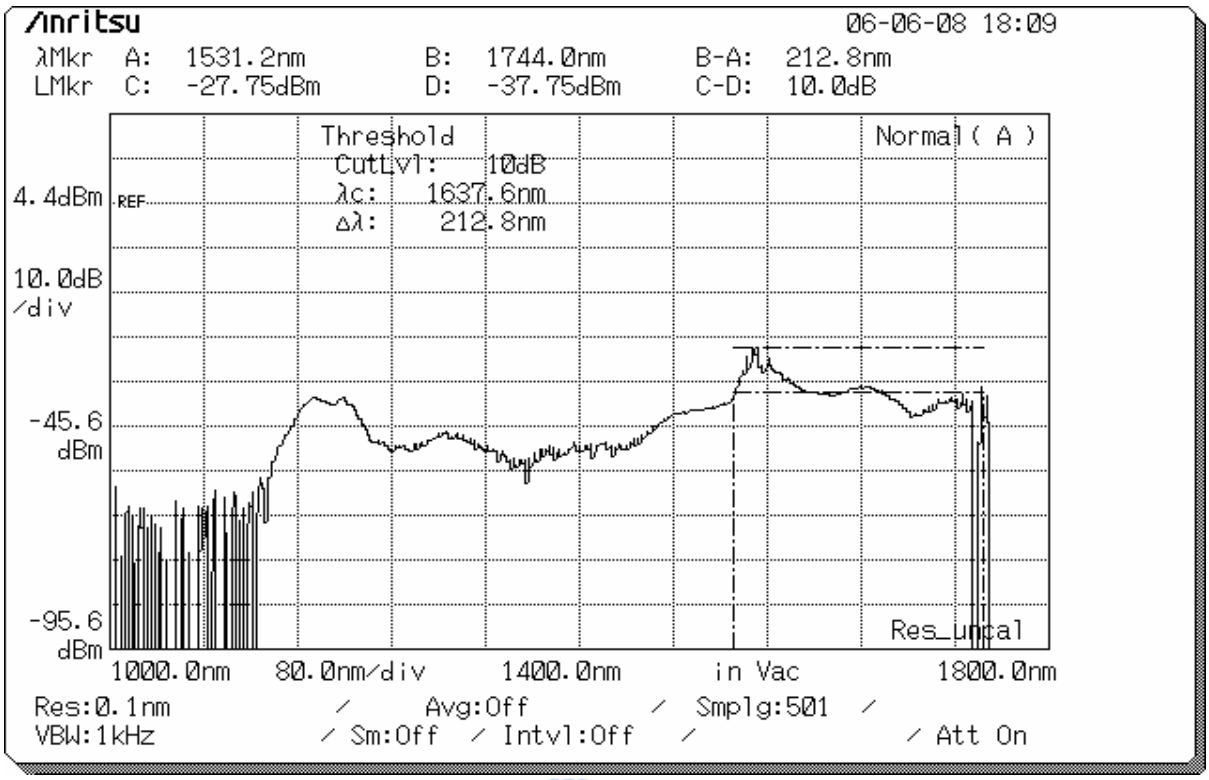

Fig 3.16 Optical spectrum of the Supercontinuum using 0.95 m HNLF-B

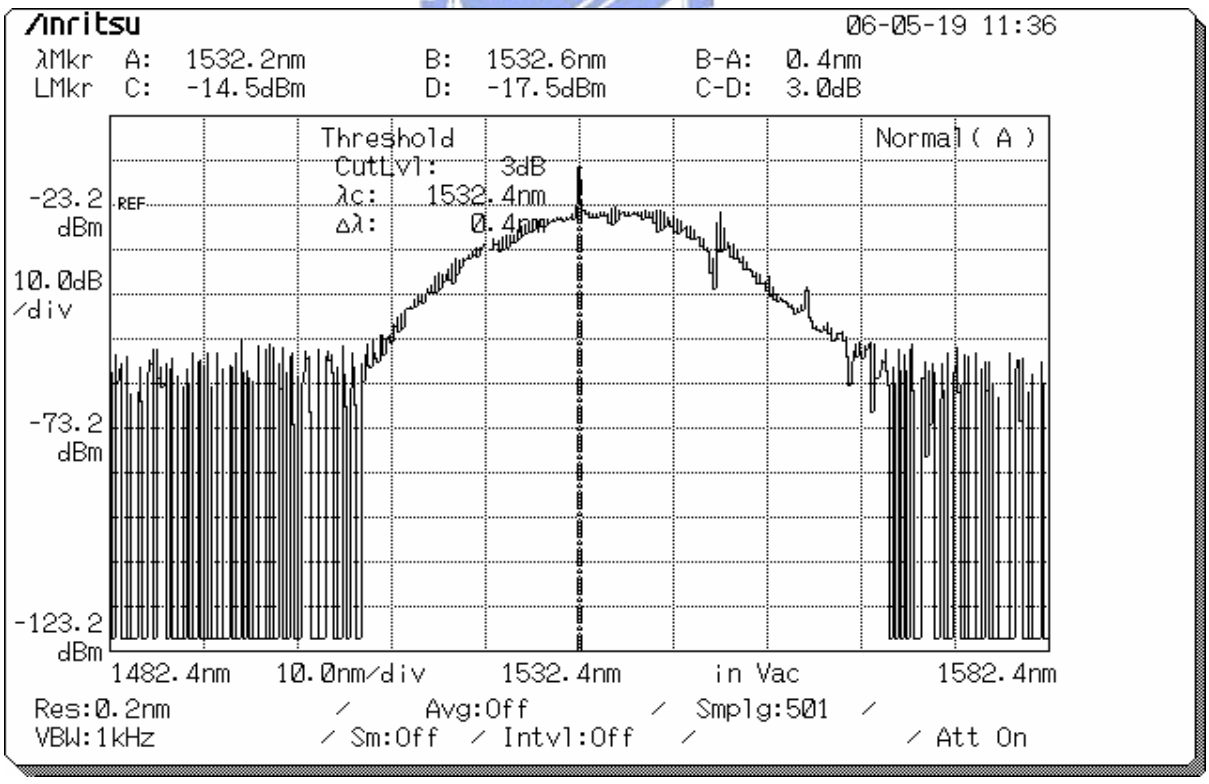

Fig 3.17 Optical spectrum of the passive mode-locked fiber laser

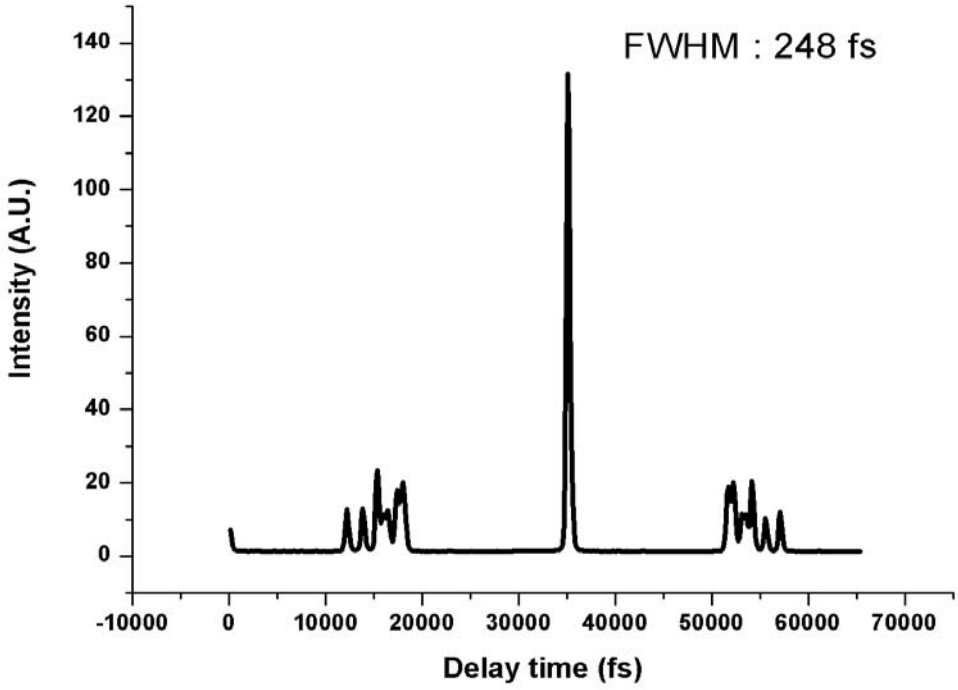

Fig 3.18 Autocorrelation of the passive mode-locked fiber laser

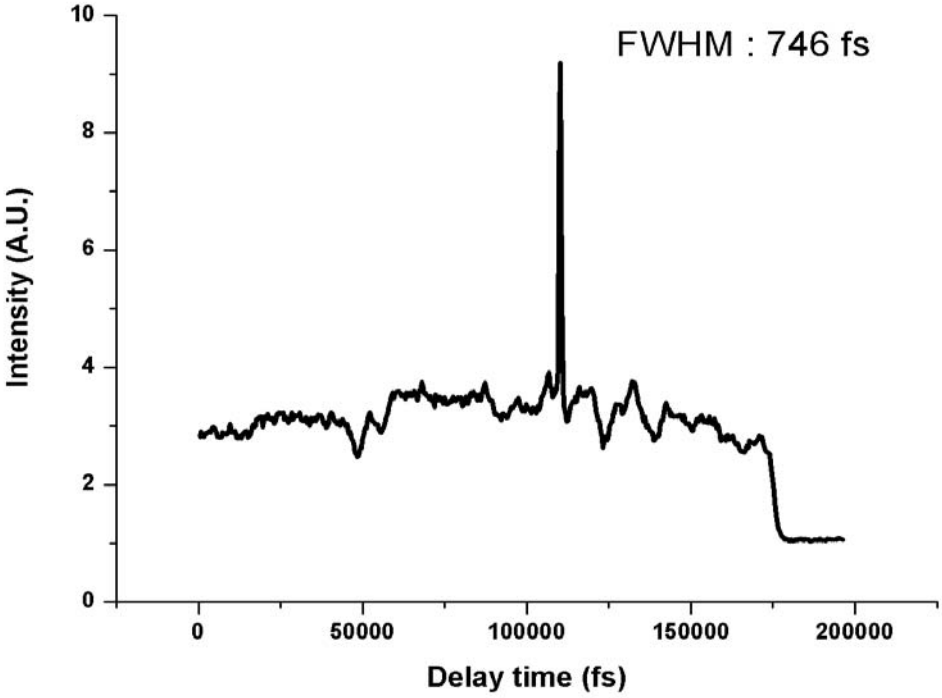

Fig 3.19 Autocorrelation of the pulse after the pulse compression

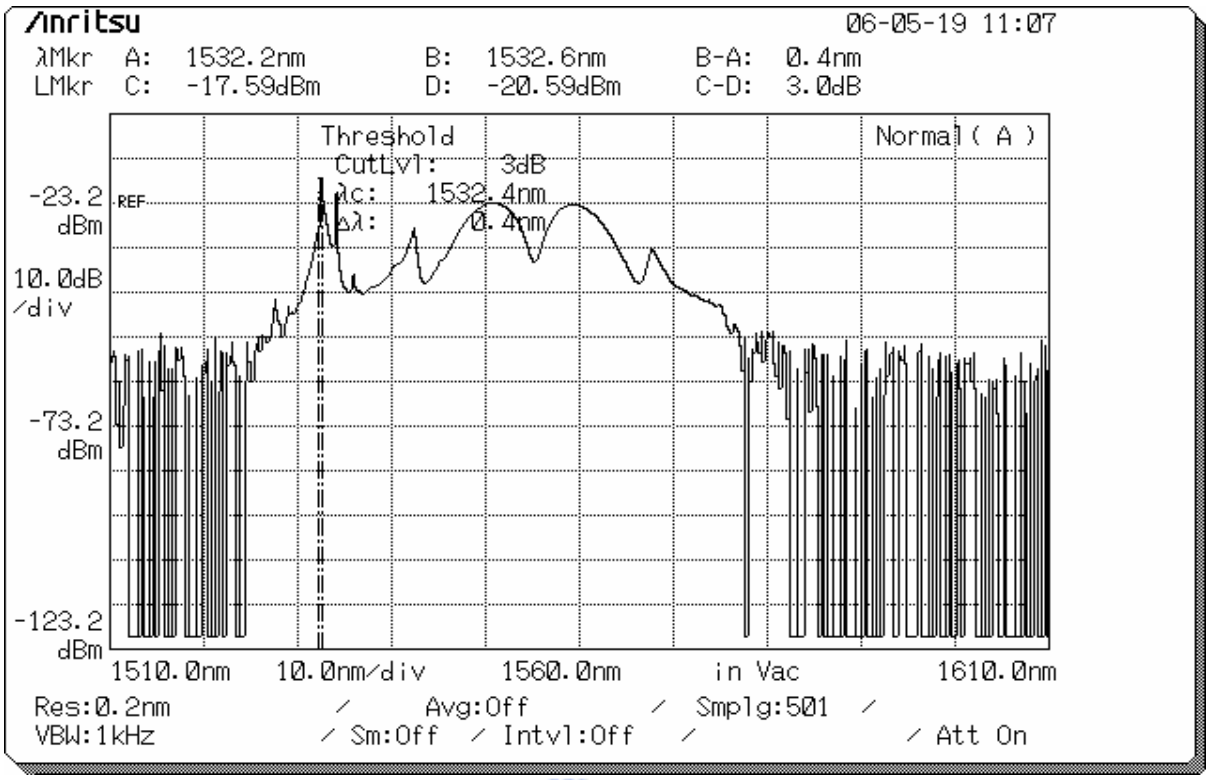

Fig 3.20 Optical spectrum of the passive mode-locked fiber laser operated at bound-state

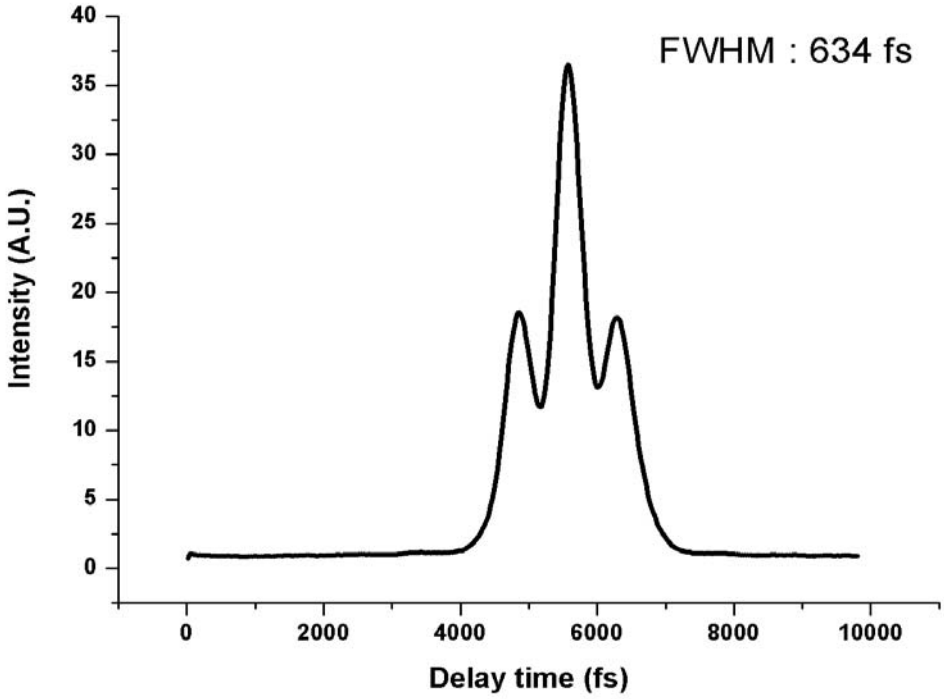

Fig 3.21 Autocorrelation of the passive mode-locked fiber laser operated at bound-state

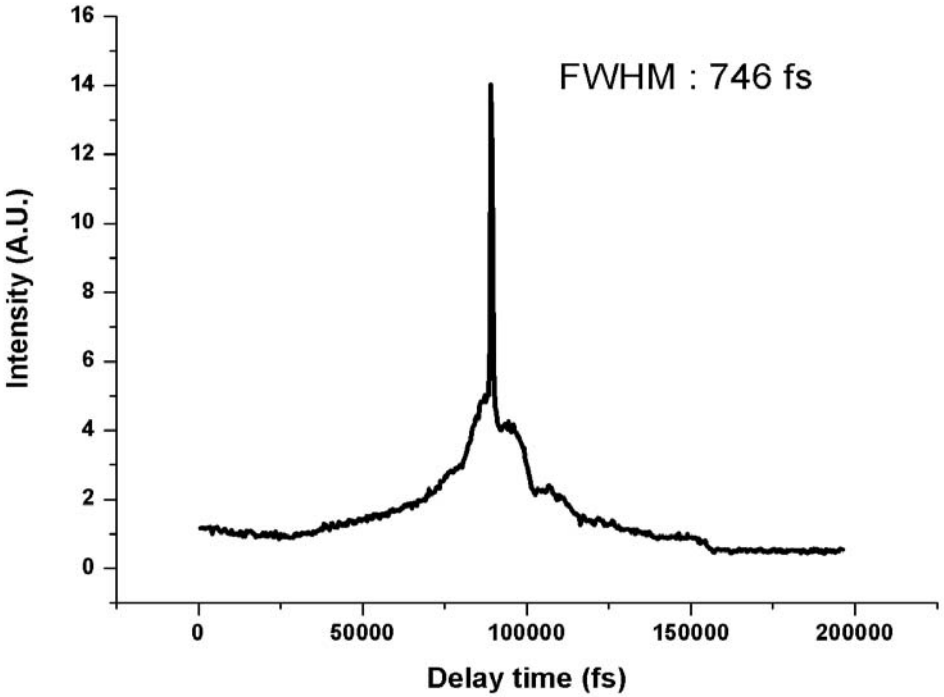

Fig 3.22 Autocorrelation of the pulse after the pulse compression：using the passive mode-locked fiber laser operated at bound-state

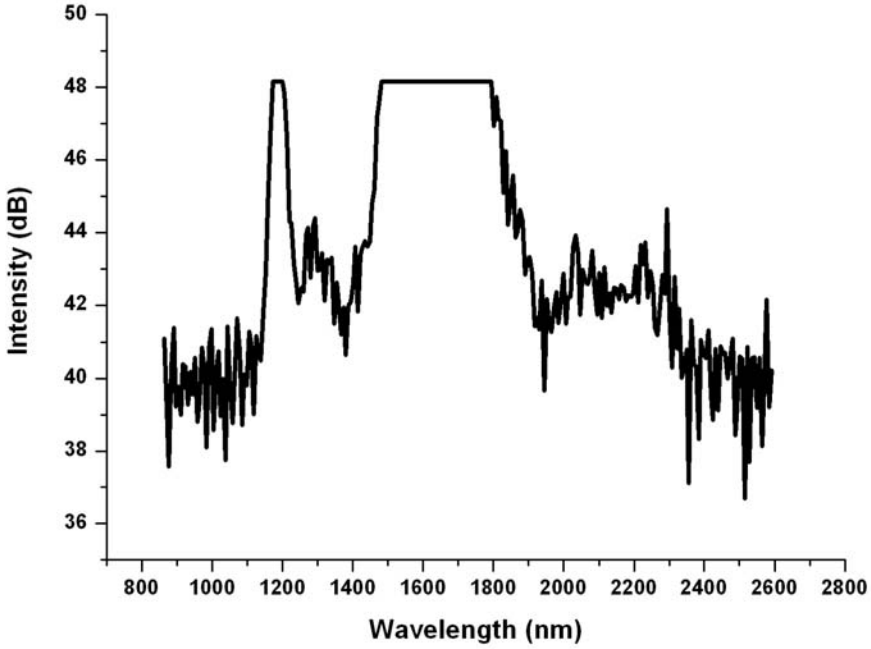

Fig 3.23 Optical spectrum of the Supercontinuum using 0.95 m HNLF-B (another optical spectrum analyzer)

Chapter 4 Conclusions and Future Work

4.1 Conclusions

In this thesis, we have demonstrate a supercontinuum light source which is composed of an ASM fiber laser, a high power optical fiber amplifier, and a section of HNLF. The ASM fiber laser which can usually be stabilized for about half a day is operated at a repetition rate of 1 GHz and generates 1.8 ps pulse train with 14 mW average power. The pulses from the ASM fiber laser propagate through a section of 1.6 m SMF which is used to introduced the chirp and then are launched into a high power optical fiber amplifier with a length of 10 m Er-Yb cladding pump fiber pumped by a 6 W laser diode at 980 nm. After amplification, the average power is risen to 1.2 W. However, the pulse train has also been broaden by the fiber amplifier. Hence, we use another SMF with the length of 25 m to achieve pulse compression, and the pulse train are successfully compressed to 414 fs. Finally, we launch the compressed pulses into a section of HNLF with the length of about 0.95 m and generate the supercontinuum light. We observe that the optical spectrum of the supercontinuum light spans from 1120 nm to 2300 nm. These results indicate that our ASM fiber laser has the potential to be the light source for high repetition rate supercontinuum generation.

4.2 Future Work

As mention before, the results of supercontinuum generation is strongly affected by the nonlinear effects from the interaction between intense optical fields and the medium. Therefore, in principle the performance can be improved by the following ways：

(1). Using a light source with shorter pulses

(2). Rising the input pulse energy

(3). Adjusting the length of HNLF

In the future, we will also establish a simulation program for numerical analysis so that we can adjust our experimental setup more precisely to generate the supercontinuum light more efficiently by using our fiber laser system.

References

[1] Y. Sun, S. Jian, S. B. Lee, K. Okamoto, “Analysis of supercontinuum generation in highly nonlinear fibers pumped by Erbium fiber laser sources: observations and optimizations,” *Proc. of SPIE*, Vol. **5623**, (2005).

[2] W. L. Smith, P. Liu, and N. Bloembergen, “Superbroadening in H_2O and D_2O by self-focused picosecond pulses from a YAlG:Nd laser,” *Phys. Rev. A*, Vol. **15**, No. 6, pp. 2396-2403, (1977).

[3] R. L. Fork et al., “Femtosecond white-light continuum pulses,” *Opt. Lett*., Vol. **8**, No. 1, pp. 1-3, (1983).

[4] R. Stolen, “Phase-matched-stimulated four-photon mixing in silica-fiber waveguides,” *IEEE J. Quantum Electronics*, Vol. **11**, No 3, pp. 100-103, (1975).

[5] P. L. Baldeck and R. R. Alfano, “Intensity effects on the stimulated four photon spectra generated by picosecond pulses in optical fibers,” *J. Lightwave Technol.*, Vol.**5**, pp. 1712-1715, (1987).

[6] K. Mori, H. Takara, and S. Kawanishi, "Analysis and design of supercontinuum pulse generation in a single-mode optical fiber", *J. Opt. Soc. Am. B.*, Vol.**18**, No. 12, pp. 1780-1792, (2001).

[7] J. K. Ranka, R. S. Windeler, and A. J. Stentz, “Visible continuum generation in air-silica microstructure optical fibers with anomalous dispersion at 800 nm,” *Opt. Let.*, Vol. **25**,

No. 1, pp.25 27, (2000).

[8] T. Okuno, M. Onishi, T. Kashiwada, S. Ishikawa, and M. Nichimura, "Silica-based functional fibers with enhanced nonlinearity and their applications," *IEEE J. Sel. Topics Quantum Electron.*, Vol. **5**, pp.1385 1391, (1999).

[9] D. Fan, K. Ueda, J. Lee, "Nonlinear propagation of the amplified highly chirped pulse and supercontinuum generation in microstructured optical fiber," *Proc. of SPIE* Vol. **5627** (2005).

[10] J. T. Gopinath, H. M. Shen, H. Sotobayashi, E. P. Ippen, T. Hasegawa, T. Nagashima, N. Sugimoto, "Highly Nonlinear Bismuth-Oxide Fiber for Supercontinuum Generation and Femtosecond Pulse Compression," *J. Lightw. Technol*., Vol. **23**, NO. 11, (2005)

[11] L. N. Durvasula, A. J. W. Brown, J. Nilsson, "CW 7-W, 900-nm-wide supercontinuum source by phosphosilicate fiber Raman laser and high-nonlinear fiber," *Proc. of SPIE* Vol. **5709**, (2005)

[12] A. K. Abeeluck, C. Headley, C. G. Jorgensen, "High-power supercontinuum generation in highly nonlinear, dispersion-shifted fibers by use of a continuous-wave Raman fiber laser," *Opt Lett*, Vol. **29**, No. 18, (2004)

[13] T. Morioka et al., "1 Tbit/s (100 Gbit/s X 10 channel) OTDM/WDM transmission using a single supercontinuum WDM source," *Electron. Lett.* Vol. **32**, pp. 906–907, (1996).

[14] S. T. Cundiff, J. Ye, and J. L. Hall, "Optical frequency synthesis based on mode-locked

lasers," *Rev. Sci. Instrum.*, Vol. **72**, No. 10, pp. 3749-3771, (2001).

[15] H. Takara et al., "More than 1000 channel optical frequency chain generation from single supercontinuum source with 12.5 GHz channel spacing," *Electron Lett.*, Vol. **36**, No. 25, pp. 2089-2090, (2000).

[16] K. Mori, T. Morioka, and M. Saruwatari, "Ultrawide spectral range groupvelocity dispersion measurement utilizing supercontinuum in an optical fiber pumped by a 1.5 μm compact laser source," *IEEE Trans. Instrum. Meas.*, Vol. **44**, pp. 712-715, (1995).

[17] G. P. Agrawal, *Nonlinear Fiber Optics*, Academic Press, San Diego, (2001).

[18] R. H. Stolen, and C. Lin, "Self-phase modulation in silica optical fibers," *Phys. Rev. A* Vol. **17**, No. 4, pp. 1448-1453, (1978).

[19] M. D. Levenson and N. Bloembergen, "Dispersion of the nonlinear optical susceptibility tensor in centrosymmetric media," *Phys. Rev. B*, Vol. **10**, No. 10, pp. 4447-4463, (1974).

[20] R. W. Boyd, *Nonlinear Optics*, (2003).

[21] M. E. Fermann, "Mode-locked multi-mode fiber laser pulse source," U.S. Pat. No. 5,818,630, (2005).

[22] H. A. Haus, "Mode-locking of Lasers," *IEEE J. on Selected topics in Quant. Electron.* Vol. **6**, 1173 (2000).

[23] H. Chen, G. Zhu, N. K. Dutta, and K. Dreyer, "Suppression of self-pulsing behavior in

erbium-doped fiber lasers with a semiconductor optical amplifier," *Applied Optics* Vol. **41**, pp. 3511, (2002).

[24] G. P. Agrawal, *Applications of Nonlinear Fiber Optics*, (2001).

[25] H. A. Haus, J. G. Fujiimoto, and E. P. Ippen, "Structures for additive pulse mode locking," *J. Opt. Soc. Am, B* Vol. **8**, 2068 (1991).

[26] M. C. Chan, "Hybrid Mode-locking Er-Fiber Laser," *Institute of Electro-Optical engineering in National Chiao-Tung University*, Master thesis, (2002).

[27] H. A. Haus, D. J. Jones, E. P. Ippen, and W. S. Wong, "Theory of soliton stability in asynchronous mode-locking," *IEEE J. Lightwave Technology* Vol. **14**, 622, (1996).

[28] J. W. Nicholson, A. D. Yablon, P. S. Westbrook, K. S. Feder, and M. F. Yan, "High power, single mode, all-fiber source of femtosecond pulses at 1550nm and its use in supercontinuum generation," *Optics Express*, Vol. **12**, No.13, (2004).

[29] M. Oberthaler and R. A. H¨opfel. "Spectral narrowing of ultrashort laser pulses by self-phase modulation in optical fibers," *Appl. Phys. Lett.* **63**, 1017–1019, (1993).

[30] B. R. Washburn, J. A. Buck, and S. E. Ralph. "Transform-limited spectral compression due to self-phase modulation in fibers," *Opt. Lett.* **25**, 445–447, (2000).